fire

Article

Effects of Natural Gas Substitution Rate and Diesel Injection Strategies on Performance and NO_x Emissions of Diesel–Natural Gas Dual-Fuel Engines

Chuanfu Kou [1,2,†], Xigan Chen [1,†], Shiqi Zeng [1], Jiaqiang E [1,3,*] and Yinjie Ma [1,3]

1 College of Mechanical and Vehicle Engineering, Hunan University, Changsha 410082, China
2 Guangxi Yuchai Machinery Co., Ltd., Yulin 537000, China
3 Institute of New Energy and Energy-Saving & Emission-Reduction Technology, Hunan University, Changsha 410082, China
* Correspondence: ejiaqiang@hnu.edu.cn
† These authors contributed equally to this work.

Abstract

Background: As global environmental issues and the energy crisis continue to intensify, diesel–natural gas dual-fuel engines have been extensively studied due to their stable combustion, low emissions, abundant natural gas reserves, and relatively low cost. **Methods**: Based on a modified YCK15 six-cylinder heavy-duty diesel engine, the experiments and GT-SUITE v2016 simulation were used to study the effects of NG substitution rate (NGSR) and diesel injection timing (DIT) on the combustion characteristics, power and emission performance of a diesel–NG dual-fuel engine running at 1800 rpm, with NGSR ranging from 0 to 50% and DIT ranging from 5 °CA BTDC to 17 °CA BTDC under four engine load conditions: 100%, 75%, 50% and 25%. **Significant Findings**: The results showed that the NGSR and DIT have considerable impact on performance enhancement and emission reduction. As NGSR increased, cylinder pressure decreased under high load and increased under low load. Under four loads, the temperature inside the cylinder revealed a downward trend, and the power and indicated thermal efficiency (ITE) decreased slightly, with power and ITE declining by less than 5% and 2%, but the fuel economy and emissions were well improved. Compared to 50% NGSR and pure diesel condition, brake-specific fuel consumption (BSFC) decreased by 5.63%, 4.60%, 2.98%, and 1.83%, respectively, and NO_x emissions decreased by 32.68%, 36.41%, 37.90%, and 38.99%, respectively. As DIT increased, cylinder pressure and temperature both increased under all four load conditions, and the power and ITE improved significantly, but this caused an increase in NOx emissions. Compared to DIT of 17 °CA BTDC with 5 °CA BTDC, power increased by 8.29%, 9.76%, 13.38%, and 16.51%, respectively, and ITE increased by 7.69%, 8.77%, 11.46%, and 12.77%, respectively. The response surface was established and performance optimized using the design of experiments (DOE) module in GT-SUITE v2016. At an NGSR of 50% and 100% loads, the optimized power was 0.431% higher than the pure diesel mode, ITE was 0.396% higher, brake-specific fuel consumption was reduced by 7.397%, and NO_x emissions were reduced by 27.027%.

Keywords: dual-fuel engine; NG substitution rate; diesel injection timing; performance enhancement; emission reduction

Check for updates

Academic Editors: Wei-Cheng Wang and Huaming Dai

Received: 29 May 2026
Revised: 26 June 2026
Accepted: 10 July 2026
Published: 13 July 2026

1. Introduction

With the development of the economy and the continuous advancement of science and technology, automobiles have become a part of everyday life for millions of households. However, the large number of internal combustion engine vehicles in use also exacerbates environmental problems [1,2]. For a considerable period of time in the future, internal combustion engines will continue to play a significant role in the field of transportation [3,4]. To address environmental pollution and energy crises, and driven by emissions regulations, the automotive industry has been undergoing continuous reform, with global energy use shifting toward more efficient and cleaner sources [5,6]. Natural gas, as a relatively ideal clean energy source, offers advantages such as large reserves, a high hydrocarbon (HC) ratio, high octane number, low emissions of pollutants after combustion, and relatively low cost. As an alternative fuel for engines, it possesses considerable potential [7]. However, the direct compression ignition of NG is challenging owing to its high auto-ignition temperature, so when traditional engines use NG as an alternative fuel for combustion, the ignition source becomes a very important factor [8]. Professor Philip proposed a method of using diesel to ignite NG. By modifying the injector, he enabled NG and diesel to be injected into a cylinder simultaneously at the end of the compression stroke, when temperature and pressure inside the cylinder are very high. The diesel can then be ignited directly by compression, and the burning diesel can ignite the surrounding NG, thereby solving the problem of NG being difficult to ignite by compression. This theory is known as high-pressure direct injection (HPDI) [9]. However, owing to extremely high structural design requirements for injectors and the complexity and high cost of the injection system associated with HPDI technology, engineers proposed diesel pilot ignition (DPI) technology for NG. Unlike HPDI, this technology does not directly inject NG into the cylinder and does not require a high-pressure common rail system. Instead, it directly injects NG into intake port, where it mixes with air and is then ignited by diesel injected into the cylinder [10]. This substantially reduces the cost of the injection system and requires minimal modification to the original diesel engine, necessitating only the addition of an NG injection system. The resulting diesel–NG dual-fuel engine can achieve both DPI combustion and pure diesel combustion, improving the reliability and adaptability of the engine [11].

It is precisely these advantages that have greatly stimulated interest in research into diesel–NG dual-fuel engines. Comparative studies have established that NG is a cleaner alternative to diesel due to the lower CO_2 emissions in dual-fuel mode, while diesel combustion produces several orders of magnitude higher NO_x and particulate emissions [12–14]. Zhang et al. [15] found that increasing the co-combustion ratio raised HC and CO emissions but greatly reduced smoke emissions. Wei et al. [16] confirmed that dual-fuel mode significantly lowers NO_x, CO_2, and PM emissions, though HC and CO may increase by several times. Mirosław et al. [17] demonstrated that dual-fuel operation significantly reduced fuel consumption and CO_2 but increased CO, HC, and NO_x concentrations.

A substantial body of literature has established that NGSR has great impact on dual-fuel engines [18,19]. In terms of combustion characteristics, Wang et al. [20] showed that at 50% load, increasing NGSR gradually decreased thermal efficiency and cylinder pressure, and the heat release rate (HRR) was fastest at 70–90% substitution and most unstable at 30–60%, with the dominance of premixed and diffusion combustion varying with NGSR. Yousefi et al. [21] reported that at 60% NGSR under low load, peak combustion temperature and NO_x declined, but unburned HC rose due to fuel overflow. Papagiannakis et al. [22] and Ahmad et al. [23] consistently found that higher NGSR lengthened ignition delay, reduced HRR, and decreased peak cylinder pressure, brake power, and exhaust temperature. Lee et al. [24] observed extended ignition delay and reduced high-temperature region volume at NGSR of 30–85%, indicating cleaner combustion trends at high substitution rates. Shu et al. [25] coupled a simplified chemical kinetics mechanism and reported that combustion duration first increased then decreased with rising NG energy fraction, while NO_x slightly increased and CO first increased and then decreased. Zhou et al. [26] found that higher NGSR shortened combustion duration and increased peak pressure, while sharply reducing soot emissions due to a more uniform air–fuel mixture and a reduction in local fuel enrichment area. Regarding overall performance and emissions, Cheenkachorn et al. [27] and Lounici et al. [28] reported that dual-fuel mode reduced ITE, volumetric efficiency, BSFC, NO_x, CO_2, and soot but elevated HC and CO. Chen et al. [29] observed that in an NG–diesel rotary engine there is higher NGSR accelerated flame propagation and improved combustion efficiency, reducing CO and soot but increasing NO_x and CO_2. Abdelaal et al. [30] found that dual-fuel engines showed significant improvements in NO_x and PM emissions, but they resulted in lower ITE and higher CO and HC emissions. Implementing EGR can address these issues and further reduce NO_x emissions. Neeraj et al. [31] found improved BSFC and BTE with reduced NO_x at 40–80% NGSR across engine speeds, but HC and CO increased. Pankaj et al. [32] showed that a 20% substitution rate decreased NO_x by 14.24% and CO_2 by 30%.

A number of studies have demonstrated that DIT also has a considerable impact on the combustion and emissions of dual-fuel engines [33–36]. Shu et al. [37] and Roussos et al. [38] demonstrated that advancing DIT advances the start of combustion and 50% burn point, leading to higher peak cylinder pressure and HRR but also significantly elevated NO_x emissions. Yang et al. [39] modified a common rail diesel engine to operate in dual-fuel mode. Research indicated that advancing DIT from 8 °CA BTDC to 17 °CA BTDC significantly improved combustion, resulting in lower HC and CO emissions. However, this led to an increase in NO_x emissions due to faster flame propagation and improved combustion phase. Therefore, appropriate DIT timing can optimize combustion and emissions in dual-fuel engines. Yang et al. [40] found that advanced DIT under low load worsened combustion noise but reduced particulate matter by up to 75%. Yousefi et al. [41,42] showed that advancing DIT increased peak pressure, ITE, and NO_x at low-to-medium loads, but NO_x began to decrease when DIT advanced beyond 30 °CA BTDC, with a maximum ITE at 46 °CA BTDC. Liu et al. [8] found that with the advance of DIT, the diesel and NG mixed more thoroughly in the cylinder, combustion duration shortened, and emissions of HC, soot and CO also reduced. Bambang et al. [43] found that the optimum DIT shifted from 17 to 15 °CA BTDC as load increased, improving thermal efficiency by 25.27% and reducing HC/CO by over 23%. Liu et al. [44] combined genetic algorithms with CFD to optimize injection strategies, indicating that optimal DIT should be delayed as diesel injection quantity increases.

In summary, extensive studies have shown that, compared to pure diesel engines, the addition of NG provides significant improvements in combustion and emission performance. Against the global backdrop of increasingly stringent emission regulations and escalating energy crises, a comprehensive investigation of the combustion and emission characteristics of diesel–NG dual-fuel engines, together with systematic optimization of their power, fuel economy, and emission performance, is of considerable practical significance.

Therefore, most existing studies have focused their analyses on a single rated operating condition, which presents significant limitations. Furthermore, systematic multi-objective optimization based on design of experiments (DOE) and response surface methodology (RSM) has rarely been applied to diesel–NG dual-fuel engines. This study focuses on the 25%, 50%, 75%, and 100% load operating ranges of diesel–natural gas dual-fuel engines. A one-dimensional thermodynamic simulation model of a diesel–natural gas dual-fuel engine was developed using GT-SUITE v2016 and validated with bench test data. This study investigated the effects of NGSR and DIT on the combustion, performance, and emissions of a diesel–natural gas dual-fuel engines. Concurrently, a multi-objective optimization method for dual-fuel engine injection parameters was developed based on DOE. With power performance, fuel economy, and emission characteristics as coordinated optimization objectives, a global optimization of injection timing and duration was completed, resulting in a comprehensive one-dimensional simulation modeling method for dual-fuel engines. By establishing and validating simulation models, exploring patterns of parameter variation, and finally performing optimization, this development process for dual-fuel engine control parameters significantly reduces the trial-and-error costs and development cycle associated with traditional bench testing, providing a standardized technical pathway for the rapid development of dual-fuel engines.

2. Models and Methods

2.1. Experimental Engine

The diesel–NG dual-fuel engine used in this experimental study was modified based on the YCK15 series six-cylinder diesel engine produced by Guangxi Yuchai Machinery Group Co., Ltd. (Yulin, China). This type of engine is commonly used in heavy-duty trucks. The main parameters of the engine are listed in Table 1.

Table 1. Main parameters of YCK15 six-cylinder diesel engine.

Parameters	Values
Engine type	Four-stroke, in-line, turbocharging
Number of cylinders	6
Displacement (L)	14.8
Bore × stroke (mm)	138 × 165
Connecting rod length (mm)	258.5
Compression ratio	22.69
Firing order	1-5-3-6-2-4
Maximum power (kW)	485
Maximum torque (N·m)	3200
Fuel injection system	High-pressure common rail

The diesel used in this study was 0# diesel, which is extensively utilized in the automotive industry. It has a high energy density, with sulfur content not exceeding 10 mg/kg, and a cetane number typically ranging from 45 to 60. The natural gas used was compressed natural gas, primarily composed of hydrocarbons, with methane accounting for over 90% of the total volume fraction of NG. The remaining portion consists of small amounts of ethane, propane, and butane, as well as hydrogen sulfide, nitrogen oxides, carbon dioxide, and trace amounts of carbon monoxide and noble gases. The physical and chemical properties of the diesel and NG are listed in Table 2.

Table 2. The physical and chemical properties of the diesel fuel and NG.

Parameters	Diesel	NG
Molecular formula	C_{10}–C_{21}	CH_4
Relative molecular mass	200–250	16
Density (g/cm^3)	0.82–0.84	0.7196
Dynamic viscosity (Pa·s)	0.003–0.008	1.1×10^{-5}–1.2×10^{-5}
Low heating value (MJ/kg)	42.5	50
Latent heat of vaporization (kJ/kg)	250–270	510
Cetane number	40–60	-
Boiling point (°C)	180–370	−161.5
Flash point (°C)	55–85	−190

Table 2. *Cont.*

Parameters	Diesel	NG
Ignition point (°C)	220	650–750
Octane number	-	130
Flame speed (m/s)	0.42	0.67
Air–fuel ratio	14.3	17.2
Auto-ignition temperature (°C)	350	537

Engine fuel injectors are classified into carburetor type, direct injection type, and intake manifold injection type based on their fuel injection methods. The engine used in this work adopted the intake manifold injection type, in which NG was injected through NG nozzles in the intake manifold. After thorough mixing with air, NG enters the cylinder. As the compression stroke nears completion, diesel is injected into the cylinder via the injector, and the NG is ignited. The parameters of the diesel injector are shown in Table 3.

Table 3. Parameters of the diesel injector used in the test engine.

Parameters	Values
Flow rate (mL/min)	2900
Nozzle number	10
Nozzle diameter (mm)	0.213
Nozzle cone angle (deg)	144
Distance from the center of the spray hole outlet to the tip of the nozzle (mm)	1
Distance from the center of the spray hole outlet to the axis of the fuel injector (mm)	1.3
Convex height (mm)	1.7
Injection pressure (bar)	1670
Back pressure (bar)	170

2.2. Mathematical Model

GT-SUITE v2016 uses various modules to simulate and calculate engine performance. Different modules include heat transfer models, fuel injection models, combustion models, etc. By adjusting the parameters in the models, the established simulation models can be made consistent with the actual engine performance. GT-SUITE v2016 employs a one-dimensional (1D) flow model for intake and exhaust manifolds and a zero-dimensional (0D) thermodynamic model for the in-cylinder process. This 0D/1D coupled approach is the standard formulation for system-level engine performance simulation, where fluid dynamics in the ducts are described by 1D conservation equations and the cylinder is treated as a spatially uniform (0D) open thermodynamic system.

2.2.1. 1D Flow Equations

In GT-SUITE v2016, the fluid dynamics of the engine model are generally described by one-dimensional fluid dynamics equations.

The continuity equation is as follows:

$$\frac{\mathrm{d}m_{\mathrm{f}}}{\mathrm{d}t} = \sum_{\mathrm{bound}} \dot{m}_{\mathrm{f}} \tag{1}$$

where m_{f} is the mass of fluid area, kg; $\dot{m}_{\mathrm{f}}$ is the mass flow through the boundary, kg/s.

The energy equation is as follows:

$$\frac{\mathrm{d}E}{\mathrm{d}t} = \frac{p_{\mathrm{f}}\mathrm{d}V}{\mathrm{d}t} + \sum_{\mathrm{bound}} (\dot{m}_{\mathrm{f}} \cdot h_{\mathrm{f}}) - \alpha_{\mathrm{g}} A_{\mathrm{f}} (T_{\mathrm{gas}} - T_{\mathrm{wall}}) \tag{2}$$

where E is fluid total energy, J; p_f is fluid pressure, Pa; dV is volume change, m^3; h_f is the specific enthalpy, J/kg; α_g is the heat transfer coefficient between the fluid and wall, W/(m^2·K); T_{gas} and T_{wall} are the gas temperature and wall temperature, K; A_f is the effective flow area, m^2.

The momentum equation is as follows:

$$\frac{\mathrm{d}\dot{m}_f}{\mathrm{d}t} = [A_f \mathrm{d}p + \sum_{\text{bound}} (\dot{m}_f \cdot u) - 4C_f \frac{\rho v^2}{2} \frac{A_f \mathrm{d}x}{D_e} - C_p(\frac{\rho v^2}{2}) A_f] / \mathrm{d}x \tag{3}$$

where u is the boundary velocity, m/s; ρ is the fluid density, kg/m^3; v is the central velocity, m/s; C_f is the surface friction coefficient, C_p is the pressure loss coefficient, D_e is the equivalent diameter, m.

2.2.2. In-Cylinder Thermodynamic Model

During the working cycle of the cylinder, the mixture inside the cylinder is treated as an ideal gas, and the working process follows the law of conservation of mass and law of conservation of energy.

The ideal gas state equation is as follows:

$$p_c V_c = m_c R_g T_c \tag{4}$$

where p_c is the gas pressure, Pa; V_c is the gas volume, m^3; m_c is the gas mass, kg; R_g is the gas constant, J/(kg·k); T_c is the gas temperature, K.

The mass conservation equation is as follows:

$$\frac{\mathrm{d}m_w}{\mathrm{d}\varphi} = \frac{\mathrm{d}m_s}{\mathrm{d}\varphi} + \frac{\mathrm{d}m_e}{\mathrm{d}\varphi} + \frac{\mathrm{d}m_k}{\mathrm{d}\varphi} \tag{5}$$

where m_w is the total mass of working fluid in the cylinder, kg; m_s and m_e are the mass of gas flowing into and out of the cylinder, kg; m_k is the mass of fuel injection, kg; φ is the crank angle.

The energy conservation equation is as follows:

$$\frac{\mathrm{d}U}{\mathrm{d}\varphi} = \frac{\mathrm{d}Q_k}{\mathrm{d}\varphi} + \frac{\mathrm{d}m_s}{\mathrm{d}\varphi} h_s - \frac{\mathrm{d}m_e}{\mathrm{d}\varphi} h_e + \frac{\mathrm{d}Q_f}{\mathrm{d}\varphi} - p_c \frac{\mathrm{d}V}{\mathrm{d}\varphi} \tag{6}$$

where U is the system internal energy, J; Q_k is the heat released by combustion of fuel in the cylinder, J; Q_f is the heat transferred into or out of each wall surface of the cylinder, J; h_s and h_e are the specific enthalpy of intake working fluid and exhaust working fluid, J/kg.

During engine operation, the energy conservation equation includes a heat transfer quantity Q_w between the engine working fluid and cylinder wall. According to Newton's heat transfer formula in heat transfer theory, Q_w can be calculated based on the instantaneous average heat transfer coefficient between the working fluid and inner wall surface α_b and the average temperature of the cylinder wall surface T_{wi}. The formula is shown below:

$$\frac{\mathrm{d}Q_w}{\mathrm{d}\varphi} = \sum_{i=1}^{3} \frac{\mathrm{d}Q_{wi}}{\mathrm{d}\varphi} = \frac{1}{\omega} \sum_{i=1}^{3} \alpha_b \cdot A_i (T_b - T_{wi}) \tag{7}$$

where φ is the crank angle, and ω is the crank speed, rad/s; A_i is the heat transfer area, m^2; T_b is the instantaneous temperature of the working fluid, K; i = 1, 2, 3 are the cylinder head, piston and cylinder liner, respectively.

Since the pressure and temperature of the working fluid inside the cylinder vary instantaneously during the working process, and due to the piston movement, the heat exchange area between the working fluid and inner wall also changes, and the amount of heat transferred through the cylinder wall at different times is also variable. Therefore, to accurately calculate the instantaneous heat transfer quantity at different times, it is necessary to correctly select α_b. In the Woschni heat transfer model, the formula for calculating α_b is as follows:

$$\alpha_b = 820P_b{}^{0.8} \cdot T_b{}^{-0.53} \cdot D_c{}^{-0.2} \cdot \left[C_1 \cdot C_m + C_2 \frac{T_a V_s}{P_a V_a}(p_b - p_0)\right]^{0.8} \tag{8}$$

where p_b and T_b are the pressure and temperature of the working fluid in the cylinder, Pa, K; D_c is the diameter of the cylinder, m; C_m is the average velocity of the piston, m/s; p_a, T_a and V_a are the pressure, temperature and volume of the working fluid at the starting point of compression, Pa, K, m^3; vs. is the cylinder working volume, m^3; p_0 is the cylinder pressure when the engine is motoring, Pa; C_1 is the gas flow velocity coefficient, and C_2 is determined by the specific configuration of the combustion chamber.

The formula for intake and exhaust phase C_1 is as follows:

$$C_1 = 6.18 + 0.417\frac{C_u}{C_m} \tag{9}$$

The formula for compression and expansion stage C_1 is as follows:

$$C_1 = 2.28 + 0.308\frac{C_u}{C_m} \tag{10}$$

where C_u is the airflow velocity, m/s; C_m is the average velocity of the piston, m/s.

2.2.3. Chemical Reaction Mechanisms of NO_x Formation

During the combustion process, the formation of NO_x is a significant issue in pollutant formation. The primary pathways for NO_x formation include thermal NO_x, prompt NO_x, and fuel NO_x. Among these, thermal NO_x is the primary source of NO_x formation under high-temperature combustion conditions. Its formation mechanism was first proposed in 1946 by Soviet scientist Yakov B. Zeldovich and was later expanded to form the extended Zeldovich mechanism, which is used to quantitatively describe the chemical kinetics of N_2 oxidation to form NO in the atmosphere at high temperatures.

Initially, it consisted of only the following two elementary reactions:

$$\mathrm{N_2{+}O} \rightleftharpoons \mathrm{NO + N(R1)} \tag{11}$$

$$\mathrm{N + O_2} \rightleftharpoons \mathrm{NO + O(R2)} \tag{12}$$

Reaction 1 is the rate-limiting step of the entire process; it requires the cleavage of an N≡N triple bond and therefore has an extremely high activation energy, which causes the reaction rate to increase significantly at high temperatures. Subsequent studies found that under fuel-rich conditions, the concentration of OH radicals rises sharply, leading to the extended Zeldovich mechanism that is widely used today:

$$\mathrm{N + OH} \rightleftharpoons \mathrm{NO + H(R3)} \tag{13}$$

Applying the steady-state approximation to N atoms (d [N]/dt $\approx$ 0), we can derive the net rate equation for NO formation:

$$\frac{d[\mathrm{NO}]}{dt} = 2k_1[\mathrm{O}][\mathrm{N}_2] \cdot \frac{1 - \frac{k_{-1}k_{-2}[\mathrm{NO}]^2}{k_1[\mathrm{N}_2]k_2[\mathrm{O}_2]}}{1 + \frac{k_{-1}[\mathrm{NO}]}{k_2[\mathrm{O}_2]+k_3[\mathrm{OH}]}} \tag{14}$$

where k_1 is the forward rate constant for reaction 1, k_{-1} is the reverse rate constant for reaction 1, and [NO] is the NO concentration.

During the initial stage of combustion or when the NO concentration is extremely low, this equation can be simplified to the following:

$$\frac{d[\mathrm{NO}]}{dt} \approx 2k_1[\mathrm{O}][\mathrm{N}_2] \tag{15}$$

As can be seen from the above equation, the formation rate of thermodynamic NO_x is primarily governed by temperature, oxygen concentration, and nitrogen concentration. This provides a direct theoretical basis for engineering-based low-NO_x combustion technologies, such as reducing peak flame temperature and controlling the excess air ratio.

2.3. Simulation Model Validation

According to the structural parameters and experimental parameters of the engine, a one-dimensional engine model can be established in the GT-SUITE v2016. The complete engine model primarily included components such as the intake manifold, intercooler, NG injector, diesel injector, cylinder, intake and exhaust valves, crankcase, exhaust manifold, turbocharger, and controller. In the software, the parameters of each module were set, and then the modules were connected to form a complete diesel–NG dual-fuel engine. The engine model is displayed in Figure 1.

Fresh air is compressed by the compressor and sent to an intercooler for cooling. The cooled air flows into the intake duct, where it is diverted into the intake manifold. In the intake manifold, air is thoroughly mixed with the injected NG to form a combustible mixture, which flows through intake valve into the cylinder and is combusted together with the injected diesel fuel. The combustion exhaust gas discharged from the cylinder is discharged through the exhaust pipe and enters the turbine to expand and do work. The turbine is connected to the compressor through a coupling, which drives the compressor to compress fresh air. This is a complete engine working cycle.

After establishing the model, it is necessary to verify and validate it. The operating conditions were specified, the simulation was executed, and the output data were compared with experimental measurements obtained from bench tests. If there is a significant discrepancy between bench test data and output results, it is imperative to re-calibrate the parameters of the modules in the engine simulation model, such as the combustion model, heat transfer model, the coefficients in the turbocharger module, etc. After making the adjustments, the simulation continues to run until the error between output results and experimental data meets the accuracy requirements needed for modeling. At that point, the simulation model is considered to be reasonably constructed and capable of meeting the requirements for subsequent simulation research.

The performance of engine model was verified and validated in terms of power, economy, and emission characteristics at a speed of 1800 rpm, 100% load, and pure diesel conditions. The cylinder pressure curve is a pivotal parameter that reflects engine operational process and evaluates its performance. The comparison with the test results is demonstrated in Figure 2, and the comparison of the results of other operating parameters is displayed in Table 4.

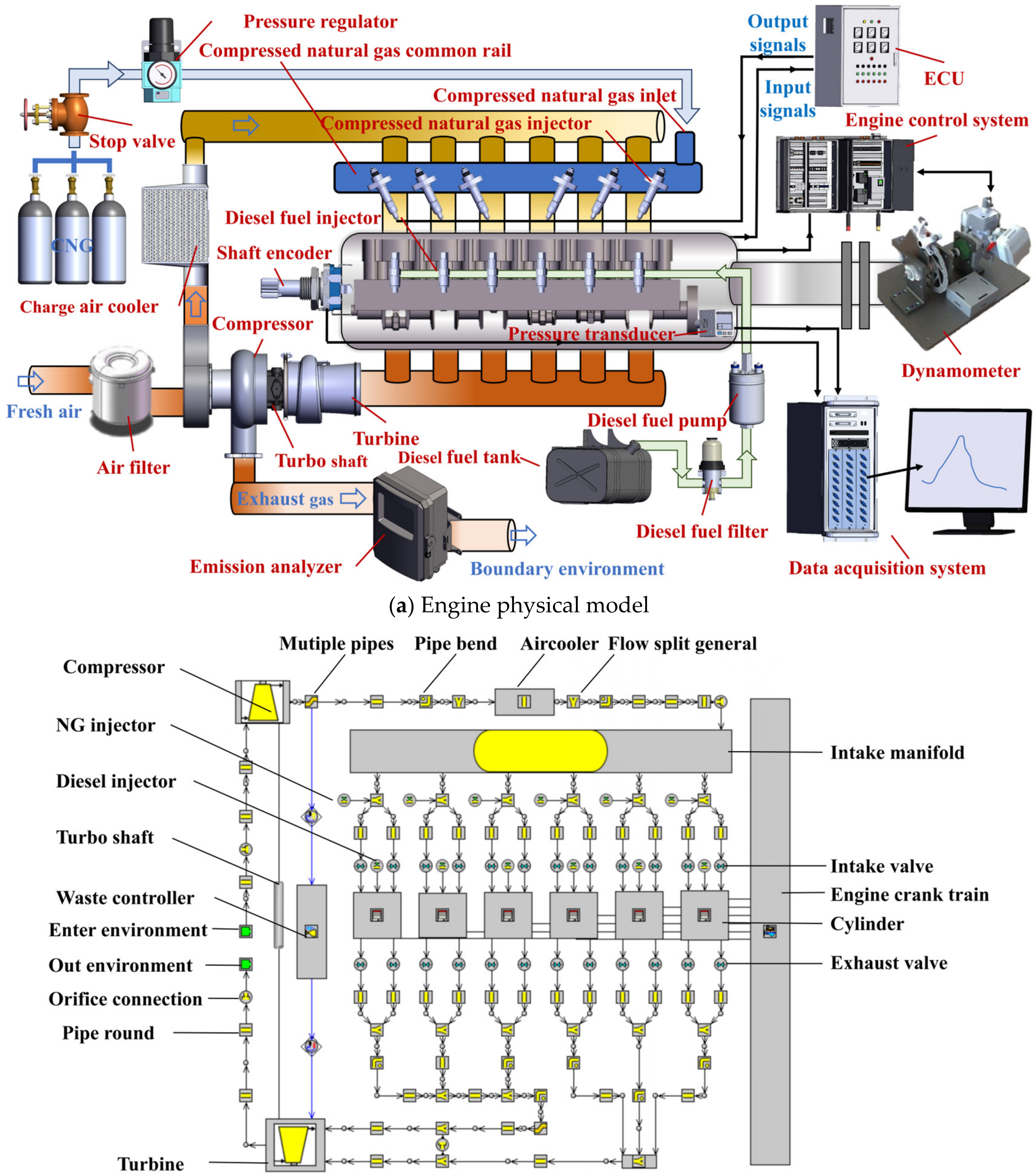

(**a**) Engine physical model

(**b**) Engine simulation model

Figure 1. Engine physical model and simulation model.

Table 4. Comparison of simulation results and experimental values for main performance parameters.

Performance Parameters	Experimental Values	Simulation Values	Error
Speed (r/min)	1800	1800	0%
Power (kW)	463.28	465.4	0.46%
Torque (N·m)	2457.7	2469.03	0.46%
BSFC (g/kWh)	204.63	203.98	0.32%
Maximum cylinder pressure (bar)	219.48	220.72	0.57%

Table 4. *Cont.*

Performance Parameters	Experimental Values	Simulation Values	Error
Intercooler inlet pressure (kpa)	307.1	308.33	0.4%
Inlet duct pressure (kpa)	302.5	302.31	0.06%
Left turbine inlet pressure (kpa)	412.82	411.02	0.44%
Right turbine inlet pressure (kpa)	461.7	456.98	1.02%
Intake temperature (K)	297.82	297.88	0.02%
Compressor outlet temperature (K)	473.31	475.66	0.5%
Intercooler outlet temperature (K)	322.12	322.76	0.2%
Intake duct temperature (K)	322.6	323.28	0.21%
Left turbine inlet temperature (K)	952.36	936.49	1.67%
Right turbine inlet temperature (K)	953.8	948.93	0.51%
Turbine exhaust temperature (K)	791.62	803.61	1.51%
NO_x emissions (ppm)	890.324	885.68	0.52%

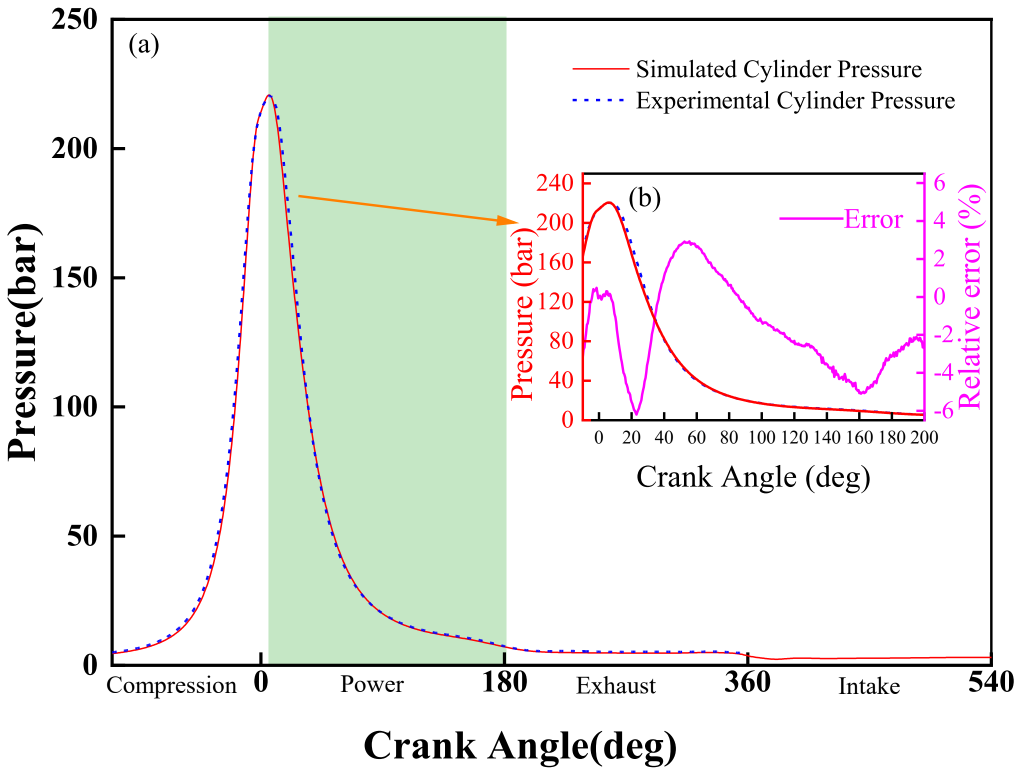

Figure 2. Comparison of in-cylinder pressure between simulation and experiment and the corresponding relative error. (**a**) In-cylinder pressure curves from simulation and experiment. (**b**) Relative error between simulated and experimental cylinder pressures, with the right vertical axis representing error percentage.

From Table 4, simulation calculation results and experimental results have an error of less than 5%, which is acceptable in engineering terms, indicating that the simulation results are reliable and the model is reasonable. Further research can be conducted on diesel–NG dual-fuel engines.

After model verification, the NGSR was studied under operating conditions of 1800 rpm and 25%, 50%, 75%, and 100% engine loads. The engine speed of 1800 rpm was selected because this is the speed at which the engine typically operates in real-world heavy-duty truck applications; it is a highly representative operating speed for evaluating the performance and emissions of the dual-fuel system under actual operating conditions. The NGSR refers to the ratio of the output energy of NG to the total output energy of diesel and NG, as shown in the following formula:

$$R = \frac{m_g \times H_g}{m_d \times H_d + m_g \times H_g} \times 100\% \tag{16}$$

where m_g is the NG injection quantity, kg; m_d is the diesel injection quantity, kg; H_g and H_d are the lower heating value of NG and diesel, J/kg.

R0 denotes an NGSR of 0%, corresponding to a pure diesel mode; R20 denotes an NGSR of 20%, at which the engine uses 20% NG energy and 80% diesel energy. The simulation study covered an NGSR range from 0 to 50%, with intervals of 10%. The NGSR range of 0–50% was selected based on the practical operating limits of the DPI dual-fuel system. Below 50% NGSR, the diesel pilot injection provides reliable ignition without requiring hardware modifications to the injection system. Above 50% NGSR, the reduced diesel quantity may compromise ignition stability and increase cyclic variability. Therefore, 0–50% represents the range within which stable dual-fuel operation can be maintained without additional engine modifications. The operating parameters are shown in Table 5.

Table 5. Engine operating parameters for the natural gas substitution rate sweep simulation study.

Speed (r/min)		**1800**		
Load (%)	25	50	75	100
Rn (%)		0, 10, 20, 30, 40, 50		
R0/Diesel (mg/hub)	95.23	161.73	227.16	292.87
R0/NG (g/min)	0	0	0	0
R20/Diesel (mg/hub)	76.19	129.38	181.72	234.30
R20/NG (g/min)	14.74	25.04	35.16	45.60
R50/Diesel (mg/hub)	47.62	80.86	113.58	146.44
R50/NG (g/min)	36.86	62.59	87.91	114

To further evaluate the applicability of the proposed dual-fuel combustion model, the simulated heat release rate at NGSRs of 50 and 100% loads was compared with published experimental results [45] obtained from a six-cylinder diesel–natural gas dual-fuel engine employing the same combustion strategy, namely natural gas port injection combined with pilot diesel direct injection. Since the present engine operated under a low in-cylinder pressure condition, the simulated results were compared with the low-pressure (n mode) case reported in the literature. As shown in Figure 3, the predicted heat release profile agrees well with the experimental trend. Both results exhibit a dominant premixed combustion stage characterized by a single major heat release peak followed by a relatively long heat release tail. Although differences remain in the absolute values of ignition delay, combustion duration and combustion phasing because of differences in engine specifications, operating conditions, boundary conditions and combustion model definitions, the overall heat release characteristics are well reproduced. This comparison provides indirect support for the applicability of the adopted dual-fuel combustion model, indicating that the model is capable of reproducing the main combustion characteristics of diesel–natural gas dual-fuel engines and is therefore suitable for investigating the effects of the natural gas substitution ratio on combustion and emission characteristics.

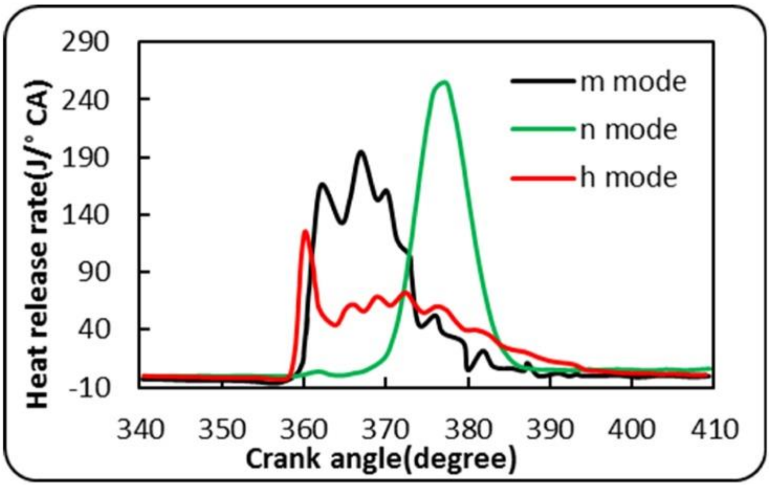

(**a**)

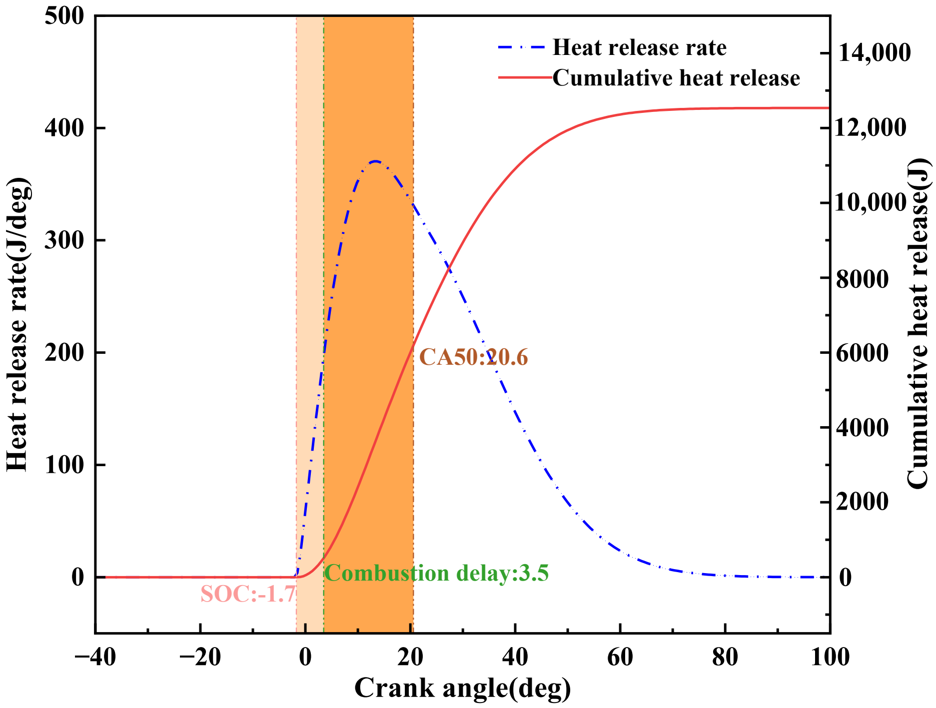

(**b**)

Figure 3. Comparison of heat release between published experimental results and simulation results. (**a**) Heat release rate of published experimental results [45]. (**b**) Heat release rate and cumulative heat release of simulation model.

3. Results and Discussion

3.1. Effect of NGSR on Engine

3.1.1. Combustion

As illustrated in Figure 4, the impact of different NGSRs on cylinder pressure is demonstrated. As the NGSR increased, the peak cylinder pressure decreased at both 100% load and 75% load. This reduction may be attributed to the increased injection quantity of NG displacing a portion of the intake fresh air, thereby leading to incomplete combustion. This causes a reduction in cylinder pressure and temperature at the end of the compression phase.

As NGSR increases, injection quantity of ignited diesel also decreases, and the penetration distance of oil jet shortens, reducing the amount of NG directly ignited by diesel, decreasing ignition area, and increasing the proportion of diffusion combustion, which reduces peak cylinder pressure. At 50% load and 25% load, as NGSR increased, the peak cylinder pressure increased slightly. This is because at lower loads, a minimal quantity of NG can mix thoroughly with air in the intake manifold to engender a more uniform mixture. A larger amount of ignited diesel allows the NG entering the cylinder to burn thoroughly. At the same time, compared to diesel, NG has a higher calorific value, releasing more heat and causing the peak cylinder pressure to rise.

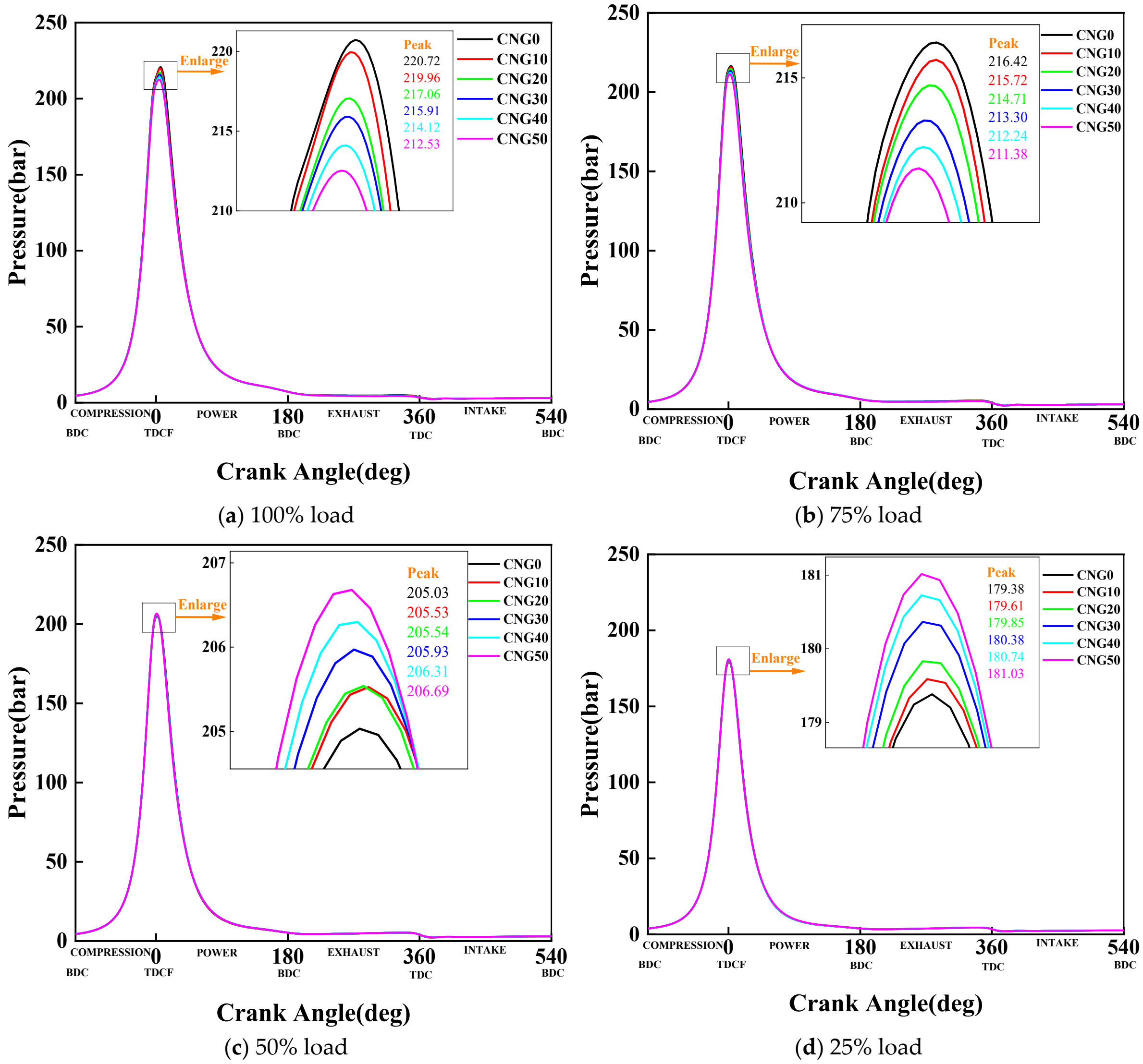

(**a**) 100% load (**b**) 75% load (**c**) 50% load (**d**) 25% load

Figure 4. Effect of natural gas substitution rate on in-cylinder pressure at (**a**) 100%, (**b**) 75%, (**c**) 50%, and (**d**) 25% engine load.

As demonstrated in Figure 5, an increase in the NGSR was observed to be accompanied by a tendency for cylinder temperature to decrease.

This is because NG occupies part of the intake manifold space, reducing the intake of fresh air. This results in a decrease in volumetric efficiency, consequently leading to a reduction in the excess air ratio and an escalation in the degree of incomplete combustion of fuel, causing the temperature inside the cylinder to decrease.

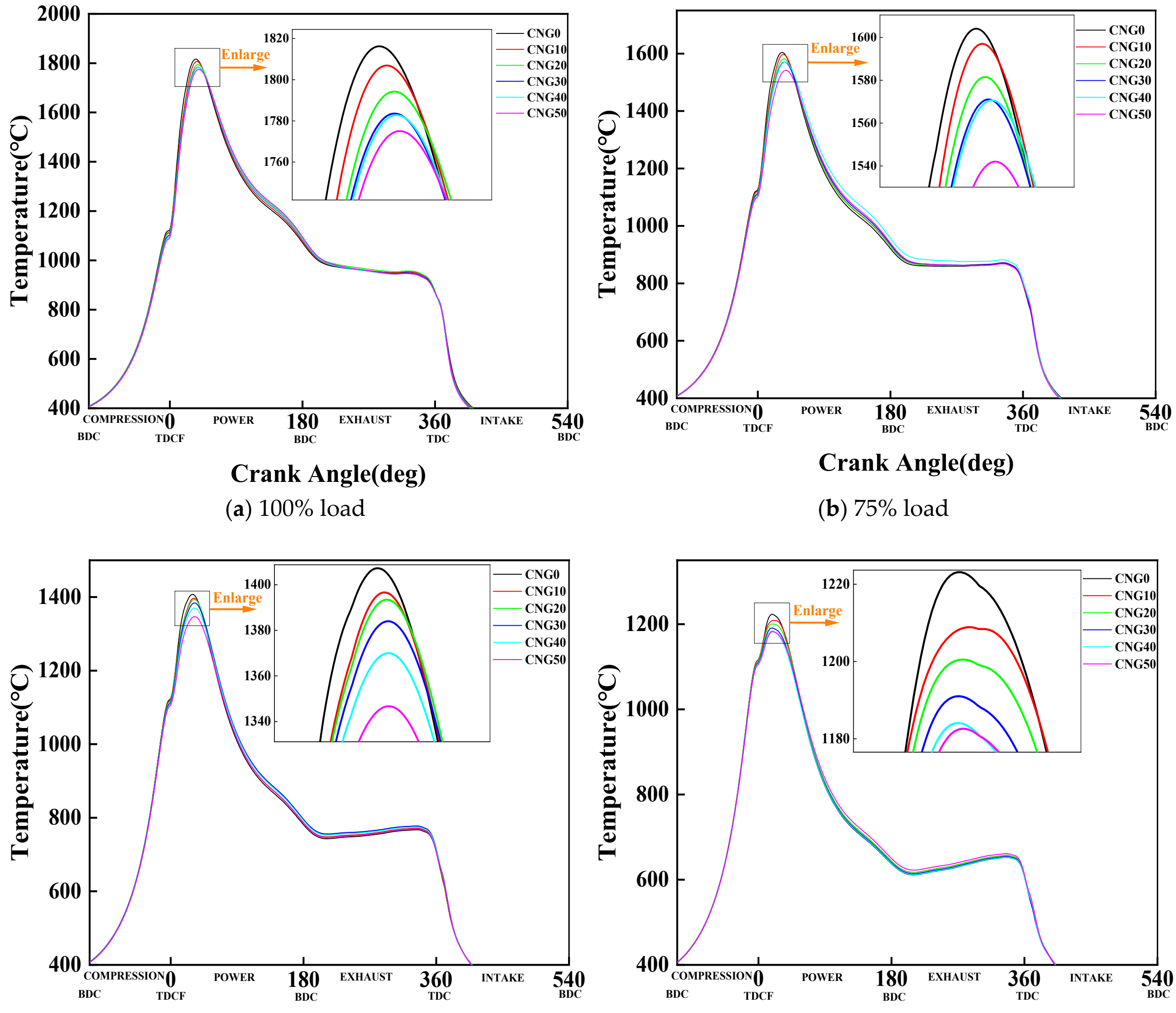

(**a**) 100% load

(**b**) 75% load

(**c**) 50% load

(**d**) 25% load

Figure 5. Effect of natural gas substitution rate on in-cylinder temperature at (**a**) 100%, (**b**) 75%, (**c**) 50%, and (**d**) 25% engine load.

3.1.2. Power Performance and Fuel Economy

The impact of NGSR on engine power is illustrated in Figure 6.

It was observed that the increase in the NGSR resulted in a slight decrease in engine power. Compared to CNG50 (a natural gas substitution rate of 50%) and CNG0 (a natural gas substitution rate of 0%), the reductions were 1.45%, 2.49%, 4.00%, and 5.03% at 100%, 75%, 50%, and 25% loads, respectively. This is because NG occupies part of the intake gas volume, reducing the pressure during the compression stage and exacerbating incomplete combustion of NG. Meanwhile, the cylinder temperature decreases. According to the Arrhenius equation, the reaction rate constant during fuel combustion decreases, resulting in an incomplete fuel reaction, less heat released, and less energy converted into mechanical energy, which results in reduced engine power.

ITE refers to the ratio of actual indicated cycle power of an engine to the heat of the fuel consumed and is an important indicator of engine performance. As displayed in Figure 7, with the growth of NGSR, ITE diminished slightly. Compared to CNG50 and CNG0, the ITE decreased by 0.595%, 0.998%, 1.547%, and 1.69% under the four load conditions, respectively. This may be attributed to the fact that NG burns more slowly than diesel. As NG injection quantity increases, combustion process is prolonged, which may cause part of the combustion to occur during the expansion stroke, thereby reducing the conversion efficiency of the effective work.

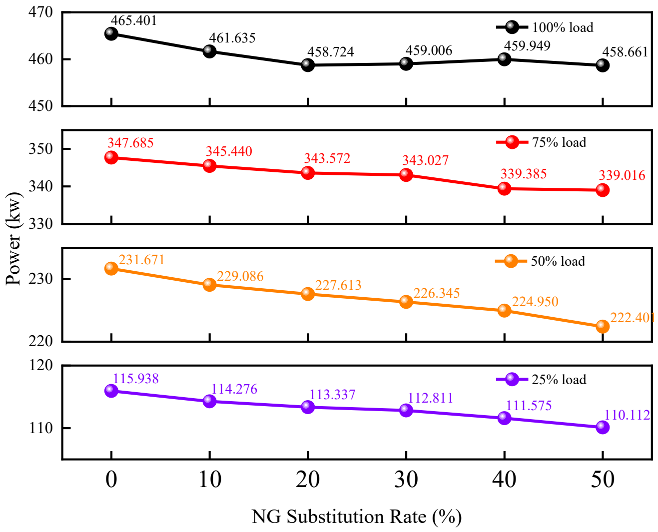

Figure 6. Effect of the natural gas substitution rate on engine power under four engine load conditions.

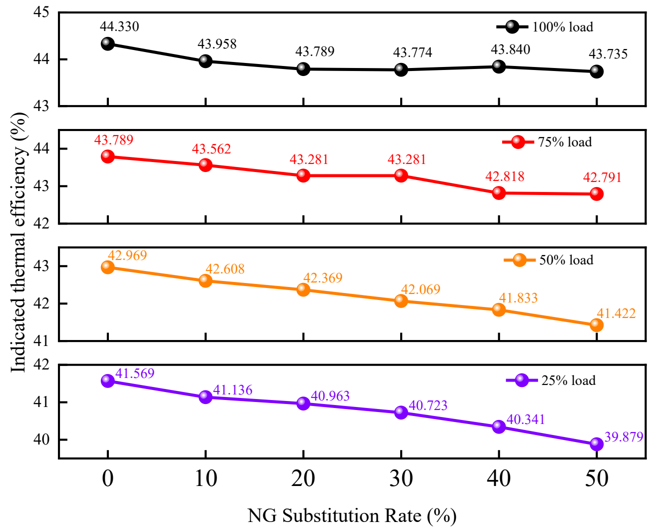

Figure 7. Effect of natural gas substitution rate on indicated thermal efficiency under four engine load conditions.

The evaluation of engine economic indicators generally focuses on BSFC. BSFC denotes the quantity of fuel utilized by an engine for each 1 kW·h of effective power output, which is defined as the amount of fuel consumed by the engine for every 1 kW·h of effective power output. The smaller the BSFC value, the less fuel the engine consumes to produce the same power and the better the fuel economy. The variation in BSFC with NGSR is shown in Figure 8.

Figure 8 shows that the BSFC of the engine exhibited a consistent downward trend in conjunction with the increase in NGSR. Compared with CNG50 and CNG0, BSFC decreased by 11.49, 9.73, 6.74 and 4.88 g/kWh, respectively, under the four load conditions. When diesel fuel is atomized, it is prone to uneven atomization, leading to incomplete combustion losses. NG, on the other hand, is premixed with air in a gaseous form, resulting in more complete combustion, thereby reducing fuel consumption.

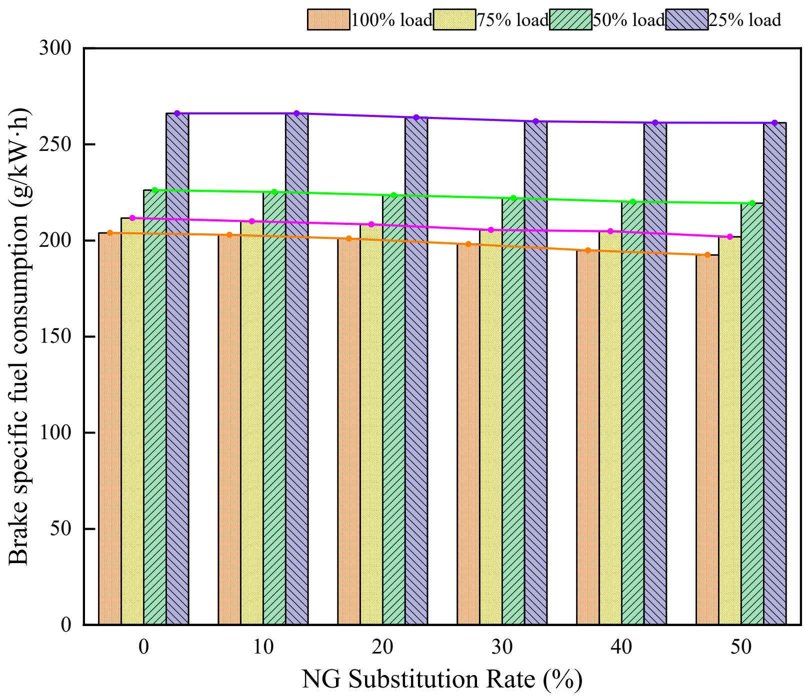

Figure 8. Effect of natural gas substitution rate on brake-specific fuel consumption under four engine load conditions.

3.1.3. Emissions

The NO_x emissions at varying NGSRs are demonstrated in Figure 9. As the NGSR increased, NO_x emissions showed a downward trend. Under four load conditions, NO_x emissions decreased by 32.68%, 36.41%, 37.90%, and 38.99%, respectively. The primary factors influencing NO_x generation are cylinder temperature, oxygen concentration in the cylinder, and sufficient reaction time. When injection quantity of NG increased, the cylinder temperature gradually decreased, which affected NO_x generation. Meanwhile, because NG accounts for a portion of the intake volume, an increased NG injection volume and reduced air flow result in a richer mixture in the cylinder and lower oxygen content, which suppresses NO_x formation and reduces NO_x emissions.

The CO emissions resulting from varying NGSRs are illustrated in Figure 10. The CO emissions exhibited a downward trend as NGSR continued to increase.

This is because CO is a product of incomplete combustion. In pure diesel mode, fuel is directly injected into the cylinder, where it mixes unevenly with the air, leading to localized oxygen deficiency and incomplete combustion. As a result, pure diesel mode produces relatively high CO emissions. As the substitution rate increases, diesel injection quantity decreases, and NG and air form a uniform mixture. The overall combustion uniformity of the mixed fuel in the cylinder is improved, resulting in more complete combustion, which reduces CO generation caused by incomplete combustion and lowers CO emissions.

CO_2 is a common greenhouse gas that has also attracted global attention. CO_2 emissions are demonstrated in Figure 11. As NGSR increased, CO_2 emissions decreased. Under four load conditions, CO_2 emissions decreased by 12.32%, 12.48%, 14.39%, and 14.34%, respectively. Compared with diesel, NG molecules contain less carbon and have a lower C/H ratio, meaning that less carbon participates in combustion.

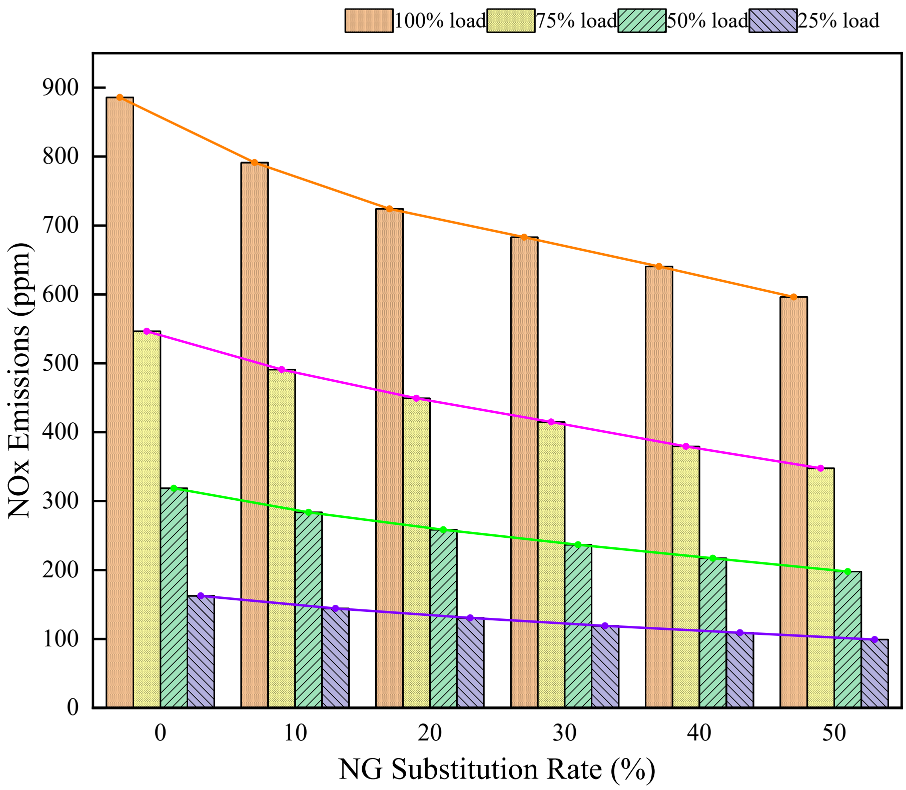

Figure 9. Effect of natural gas substitution rate on NO_x emissions under four engine load conditions.

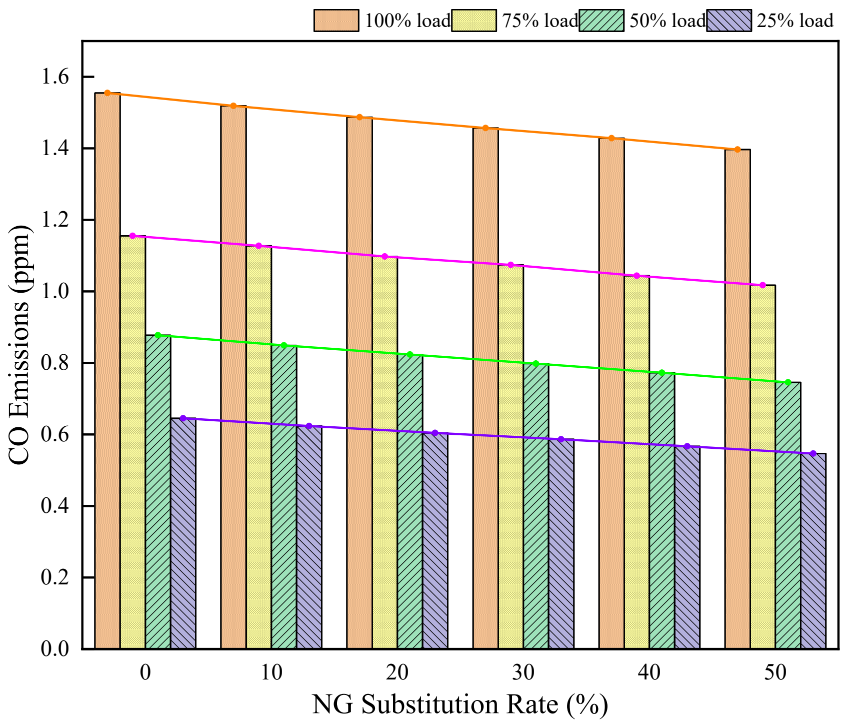

Figure 10. Effect of natural gas substitution rate on CO emissions under four engine load conditions.

According to the law of conservation of mass in chemical reactions, this results in less CO_2 being produced during combustion. Research has also shown that in dual-fuel combustion mode, fewer OH radicals are produced, which is unfavorable for oxidation of CO to CO_2; therefore, CO_2 emissions are reduced.

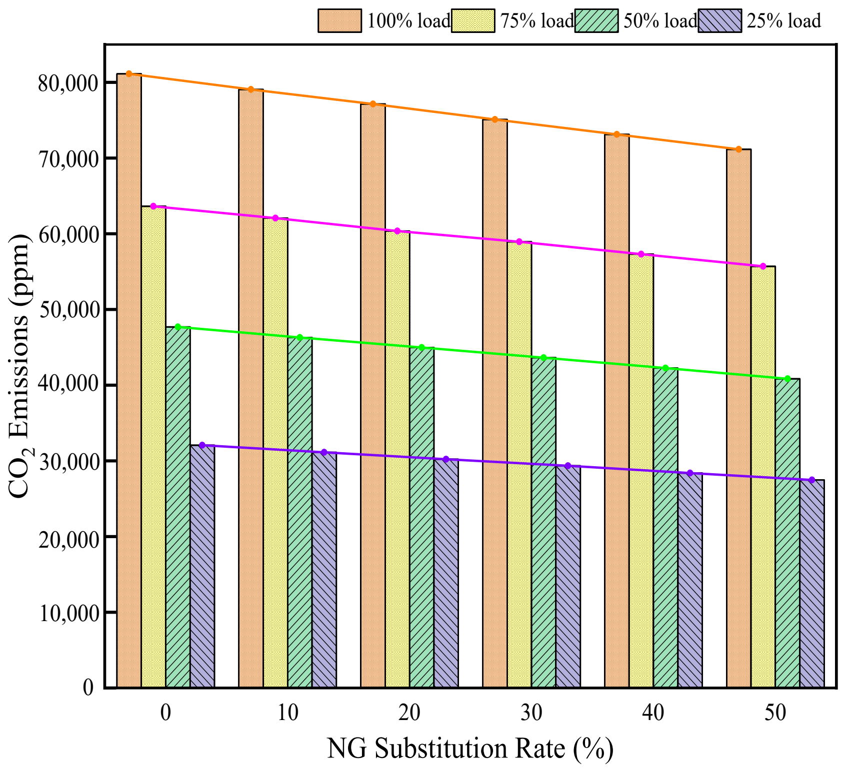

Figure 11. Effect of natural gas substitution rate on CO_2 emissions under four engine load conditions.

3.2. Effect of DIT on Engines

DIT exerts a profound influence on engine combustion, performance, and emissions. DIT determines the precise moment at which fuel enters the cylinder, affecting physical and chemical reactions such as fuel evaporation, atomization, and oxidation, thereby influencing the mixed combustion process of diesel and NG. Therefore, appropriate IT plays a crucial role in improving combustion, performance, and emissions. This section examines the effect of IT from 5 °CA BTDC to 17 °CA BTDC on engines under conditions of an NGSR of 50%, an engine speed of 1800 rpm, and engine loads of 25%, 50%, 75%, and 100%.

3.2.1. Effect of DIT on Combustion Performance of Engines

Figure 12 shows the changes in cylinder pressure inside the engine under different IT. As IT advanced, cylinder pressure showed an increasing trend. This is because when IT advances, the piston is far from the top dead center at this point, and pressure and temperature are lower. Meanwhile, there is sufficient time for the diesel to atomize, evaporate and mix with air and NG, thereby facilitating the formation of a more uniform combustible mixture. During combustion, the diesel atomizes and evaporates well, resulting in high combustion efficiency and faster combustion speed. There is sufficient ignition energy to ignite the NG, resulting in more complete combustion and increased pressure inside the cylinder. As IT was advanced, the increase in maximum cylinder pressure was relatively small under low-load conditions. This is because under low-load conditions, the quantity of fuel and air entering the cylinder is diminished, resulting in a leaner fuel–air mixture. While advancing the IT can improve ignition, the flame propagation of diesel ignition is limited, resulting in a slower overall combustion rate and a more gradual pressure rise. Additionally, due to the dilution effect, there is a higher residual exhaust gas content at low loads, which absorbs heat and lowers flame temperature, thereby slowing the combustion reaction. At high loads, the dilution effect is weaker, and combustion is more significantly influenced by IT.

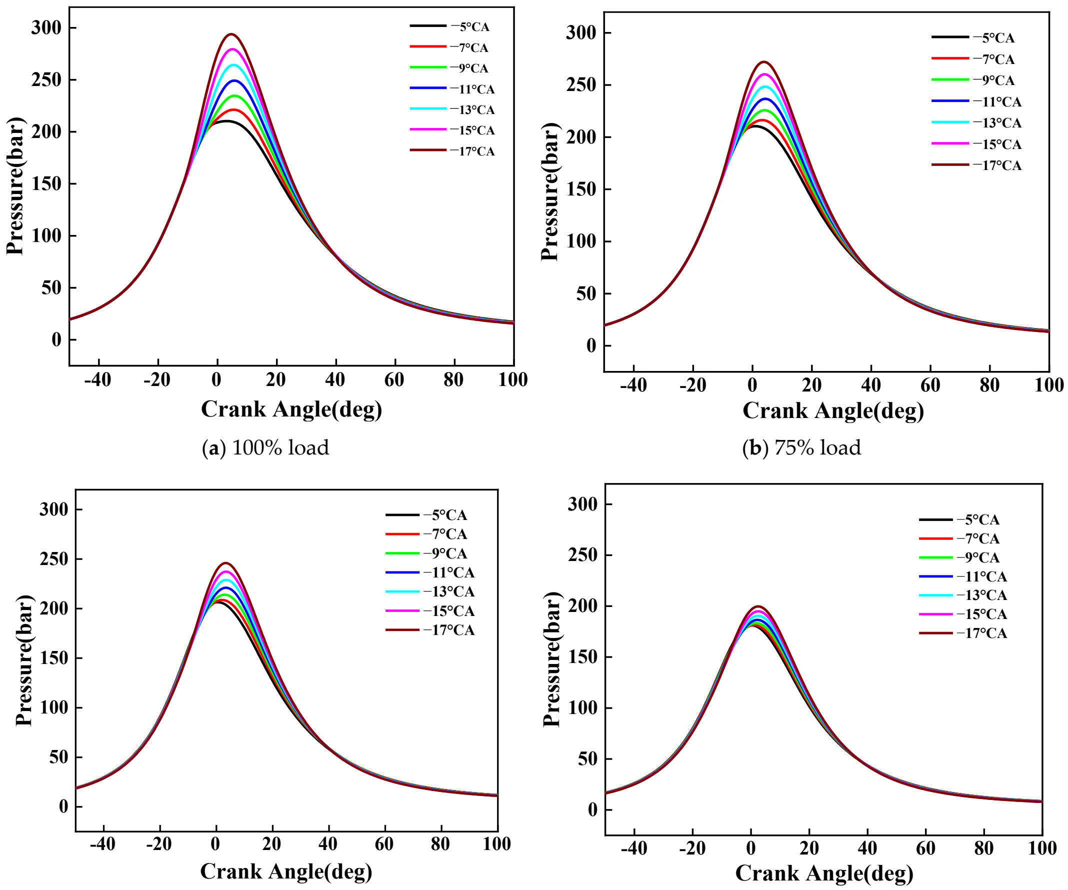

(**a**) 100% load (**b**) 75% load

(**c**) 50% load (**d**) 25% load

Figure 12. Effect of diesel injection timing on in-cylinder pressure at (**a**) 100%, (**b**) 75%, (**c**) 50%, and (**d**) 25% engine load.

Figure 13 displays the changes in engine temperature under different IT. When IT advanced, maximum cylinder temperature increased. The underlying cause of this alteration is analogous to variations in cylinder pressure. The advanced IT prolongs the ignition delay period, allowing injected diesel more time to mix with air and NG, forming a uniform mixture.

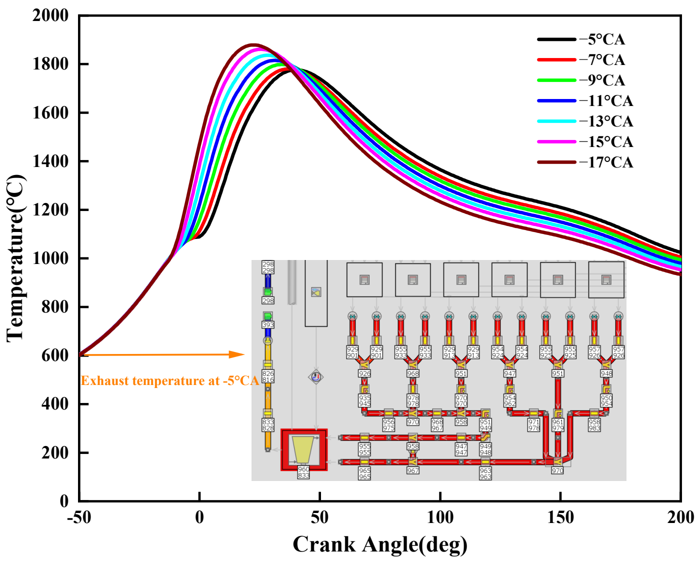

(**a**) 100% load

Figure 13. *Cont.*

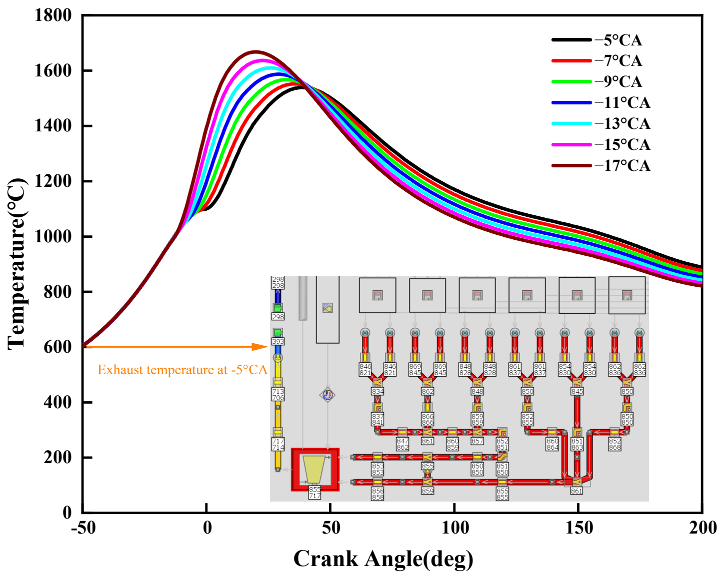

(**b**) 75% load

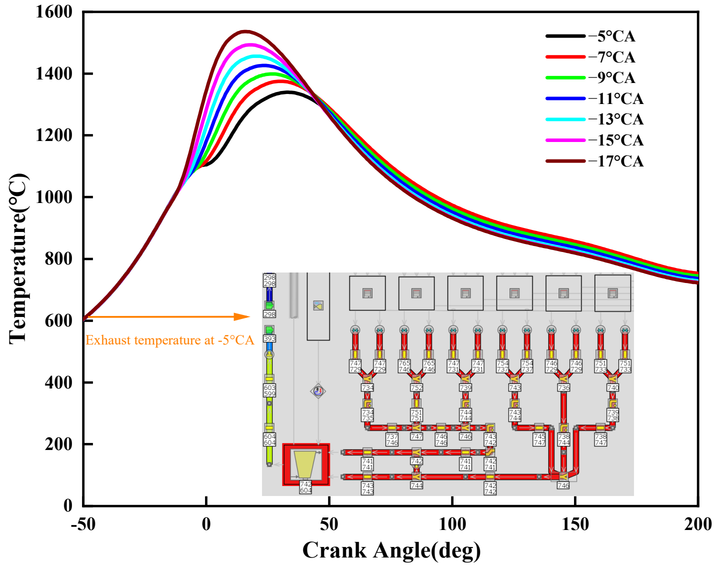

(**c**) 50% load

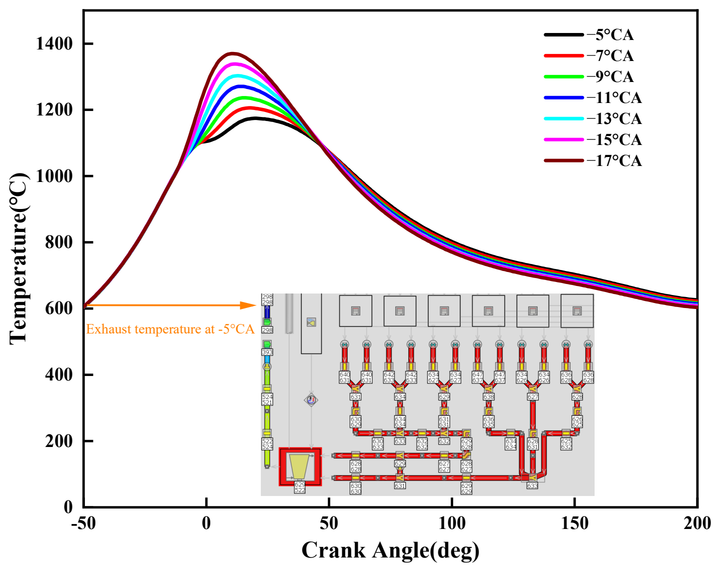

(**d**) 25% load

Figure 13. Effect of diesel injection timing on in-cylinder temperature at (**a**) 100%, (**b**) 75%, (**c**) 50%, and (**d**) 25% engine load.

During the extended ignition delay period, a substantial quantity of combustible mixture accumulates, thereby enhancing combustion efficiency and elevating in-cylinder temperature. When IT was 5 °CA BTDC, the exhaust temperature also increased with the load increase. As the load increased, the total energy of the fuel entering the cylinder also increased, and HRR also increased significantly, resulting in an increase in exhaust gas energy and temperature. The exhaust gas temperature of different engines is limited by material constraints. To prevent overheating and damage to components such as exhaust valves, exhaust manifolds and turbochargers, the exhaust gas temperature must be regulated within an appropriate safety range.

3.2.2. Effect of DIT on Power Performance and Fuel Econom Performance of Engines y

Figure 14 shows the change in power under different IT. As DIT advanced, there was a continuous increase in engine power. Under four loads, comparing IT 17 °CA BTDC and 5 °CA BTDC, power increased by 8.29%, 9.76%, 13.38%, and 16.51%. Advanced injection allows the diesel to mix thoroughly with NG, resulting in more complete combustion and the release of more energy, which is then converted into greater power output. At the same time, advanced diesel injection also creates better conditions for NG combustion, enabling the NG to be fully ignited by the diesel, thereby increasing the power output.

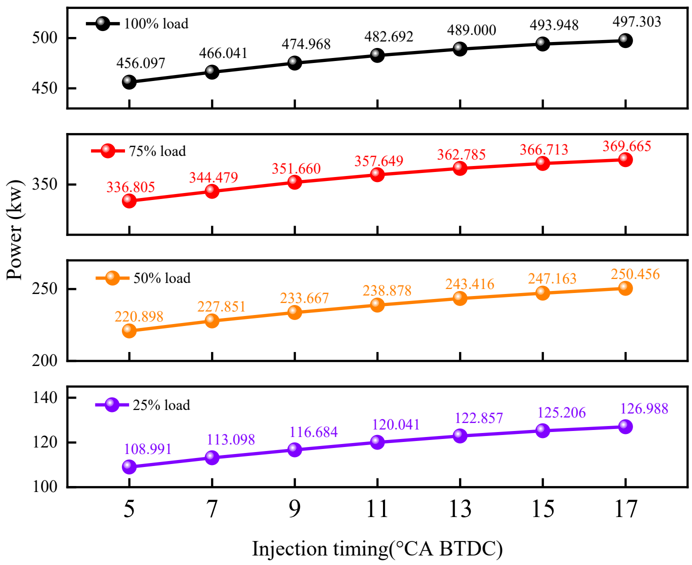

Figure 14. Effect of diesel injection timing on brake power under four engine load conditions.

Figure 15 shows the change in ITE under different IT. As IT advanced, the ITE of the engine increased. Under four loads, ITE increased by 7.69%, 8.77%, 11.46%, and 12.77%, respectively. This is because advancing the IT prolongs the ignition delay period of diesel, which is more conducive to fuel mixing and allows for the formation of a more uniform diesel–NG–air mixture. This enables the ignition of more NG, promoting complete fuel combustion and thereby increasing the ITE.

BSFC is an important indicator of engine fuel economy, directly reflecting the efficiency of fuel consumption by the engine. A lower BSFC value indicates a higher energy conversion efficiency in the engine.

As Figure 16 displays, BSFC decreased as IT advanced. Comparing IT 17 °CA BTDC and 5 °CA BTDC, BSFC decreased by 16.00, 18.04, 26.06, and 38.27 g/kWh under four loads. Advancing the IT allows sufficient time for diesel to atomize and evaporate, while also ensuring thorough mixing with fuel and air. This improves the completeness of fuel combustion, ignites more NG, reduces energy loss caused by incomplete combustion, and consequently lowers the BSFC and improves the ITE of the engine.

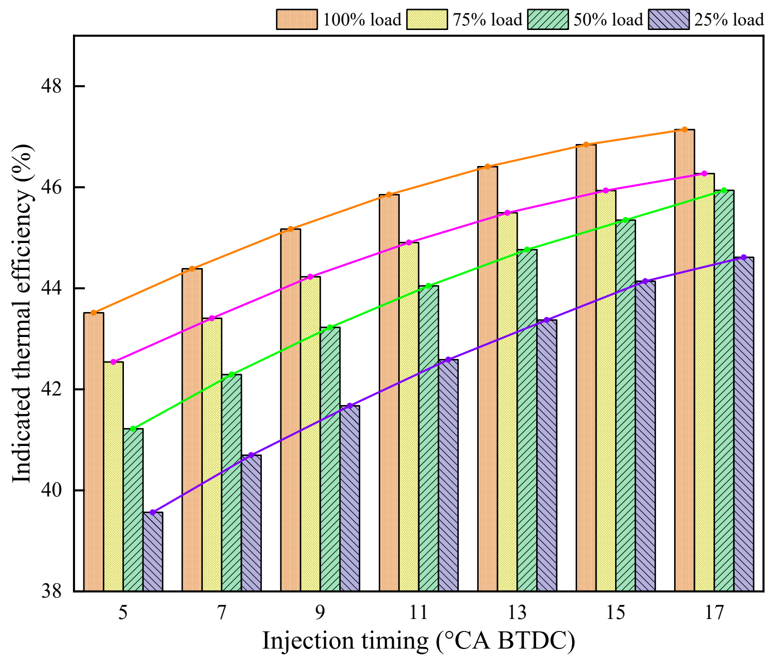

Figure 15. Effect of diesel injection timing on indicated thermal efficiency under four engine load conditions.

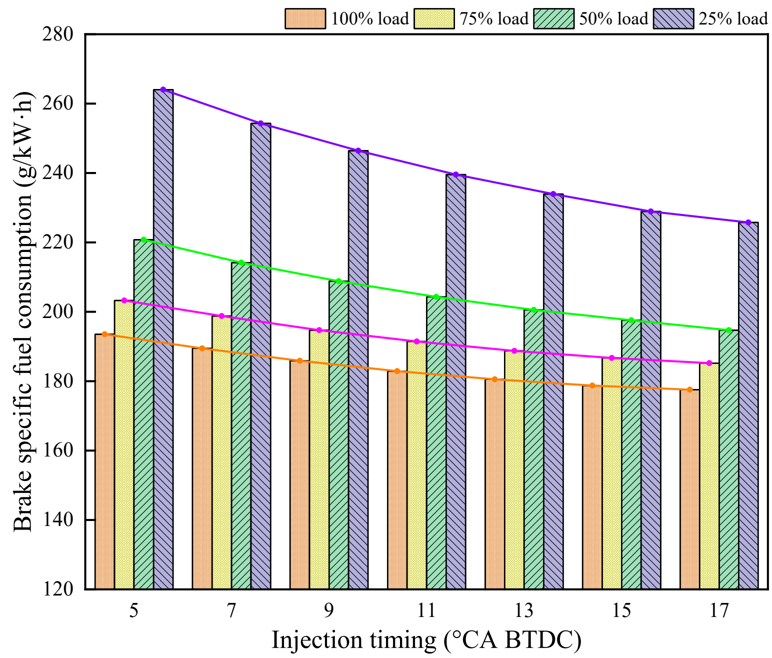

Figure 16. Effect of diesel injection timing on brake-specific fuel consumption under four engine load conditions.

3.2.3. Effect of DIT on Emissions Performance of Engines

From Figure 17, NO_x emissions increased with the advance of IT. Comparing IT 17 °CA BTDC and 5 °CA BTDC, NO_x emissions increased by 130.60%, 148.81%, 183.24%, and 186.00% under four loads, respectively. NO_x emissions are primarily related to temperature and oxygen concentration. The advancement of IT results in a longer mixing time between diesel and air–NG, leading to more complete combustion.

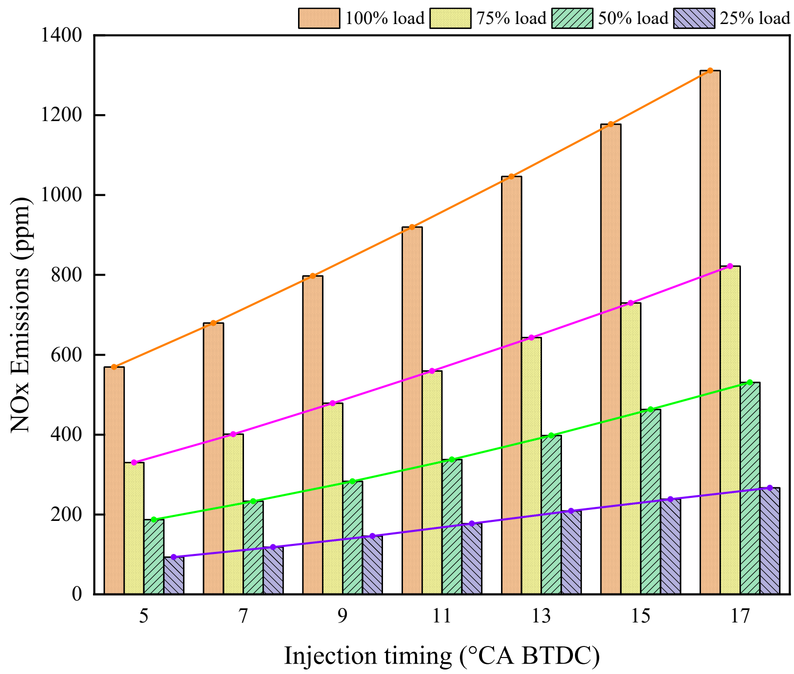

Figure 17. Effect of diesel injection timing on NO_x emissions under four engine load conditions.

This causes an increase in cylinder temperature. The Zeldovich mechanism posits that the concentration of oxygen, combustion temperature, and residence time are key factors influencing NO_x formation. An increase in cylinder temperature and uniform mixing of oxygen within the cylinder promote NO formation, resulting in increased NO_x emissions.

As displayed in Figure 18, as IT advanced, CO_2 emissions increased slightly. Under four loads, CO_2 emissions increased by 198.64, 82.06, 1318.83, 1192.66 ppm, respectively. This may be because advancing IT allows the diesel fuel to mix more thoroughly with NG and air in the cylinder, resulting in more complete combustion. Meanwhile, the higher cylinder temperature facilitates the complete oxidation of more carbon elements in the fuel into CO_2, thereby increasing CO_2 emissions.

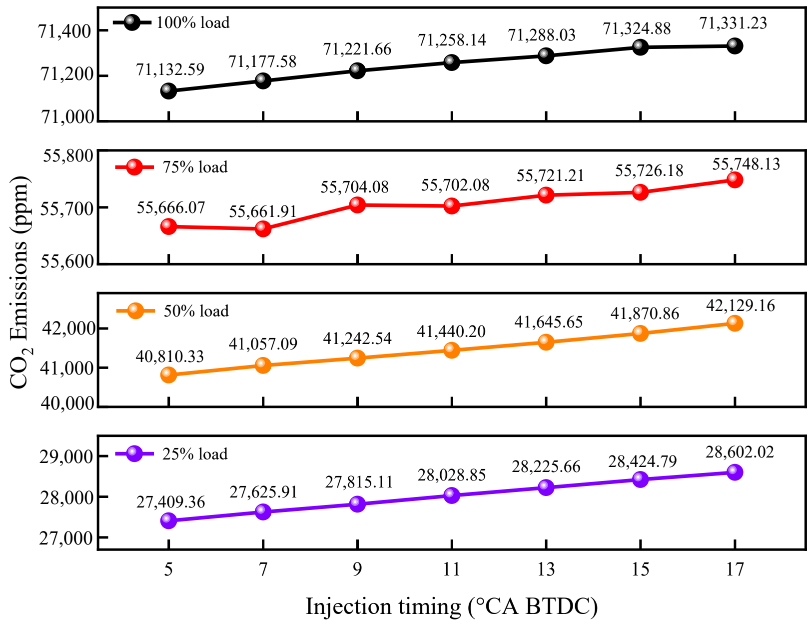

Figure 18. Effect of diesel injection timing on CO_2 emissions under four engine load conditions.

3.3. Design of Experiments

Design of experiments (DOE) is a systematic statistical methodology that enables the simultaneous investigation of multiple input factors and their interactions on one or more response variables, while minimizing the number of experimental runs required [46]. In engine calibration and optimization, DOE has largely replaced the traditional one-factor-at-a-time (OFAT) approach because it captures factor interactions and provides a global model of the system's behavior with higher efficiency. The core principle of DOE is to select a set of design points within a multi-dimensional parameter space so that the resulting data can be used to construct a reliable, typically polynomial response surface model. GT-SUITE v2016 includes a built-in DOE module. By setting and running parameters within the GT-SUITE v2016, it can be used to study the effects of multiple input parameters on multiple output results. After multiple experiments were completed in the DOE module, response surface methodology (RSM) and optimization design can be performed on the experimental results in the post-processor.

3.3.1. DOE Setup

In the DOE module of GT-SUITE v2016, there are many sampling methods, including full factorial, D-Optimum, Latin Hypercube, D-Optimum Latin Hypercube, etc. In this study, the Latin hypercube sampling (LHS) method was adopted for the generation of design points. LHS is a stratified random sampling technique that divides the range of each input variable into n non-overlapping intervals of equal marginal probability, where n is the number of design runs. From each interval, a single value is randomly sampled without replacement. This ensures that every variable's entire range is uniformly represented, even with a relatively small number of experiments. Compared to full factorial designs, which require k^n runs for k factors each at n levels and quickly become prohibitive, LHS provides excellent space-filling properties with far fewer design points. Compared to simple random Monte Carlo sampling, LHS avoids the clustering of points in certain regions and guarantees more even coverage of the parameter space. The Latin Hypercube method satisfies the uniformity and orthogonality requirements of DOE while enabling precise fitting of the response surface with a relatively small number of experiments.

In the DOE module of GT-SUITE v2016, the DIT and diesel injection duration (DID) were selected as independent variables. The upper and lower limit values of the two factors are shown in Table 6. Changes in DID affect the time distribution of fuel injection, atomization quality and air mixing efficiency. A reasonable DID can optimize combustion and emissions, so DID was selected as a parameter for collaborative optimization with DIT. DOE was performed under operating conditions of a 50% NSGA. DOE optimization was conducted at a 50% NGSR. With a significant level of diesel substitution, the project offers high economic value. Furthermore, during normal engine operation, the system runs stably at a 50% substitution rate. Combustion consists of a combination of diesel diffusion combustion and natural gas premixed combustion, demonstrating good optimization potential. At substitution rates above 50%, issues such as insufficient ignition energy, unstable ignition, and deteriorated combustion are likely to occur. Within the safe operating range, 50% is the substitution ratio that ensures stable operation without significant power loss, making it a representative and typical operating condition for DOE optimization. The DIT range for the DOE was restricted to 5–8 °CA BTDC. As demonstrated in Section 3.2, advancing DIT beyond 8 °CA BTDC at full load yields diminishing improvements in power and ITE while drastically increasing NO_x emissions. Therefore, the DIT was restricted to 5–8 °CA BTDC because this interval provides a favorable compromise between power improvement and NO_x control. This also improves the accuracy of DOE optimization. The number of experiments was 35, and Latin Hypercube sampling was performed. The resulting Latin

https://doi.org/10.3390/fire9070297

Hypercube array is shown in Table 7. Simulation experiments were conducted at NGSRs of 50% and 100% loads, and power, ITE, BSFC, and NO_x emissions were selected as responses. The DOE experimental results are also shown in Table 7.

Table 6. Upper and lower limits of factors.

Factor	Lower Limit	Upper Limit
Injection timing	−8	−5
Injection duration	6	20

Table 7. Latin Hypercube sampling array and the corresponding simulation responses at 50% NGSR, 100% load.

	Injection Timing	Injection Duration	Power (kW)	ITE (%)	BSFC (g/kW·h)	NO_x (ppm)
1	−5.75493	12.3628	458.792	43.7429	192.451	604.113
2	−7.56571	14.2899	467.716	44.5303	188.777	703.305
3	−5.23379	18.0949	456.382	43.529	193.473	577.681
4	−6.27329	8.57325	461.362	43.9719	191.369	630.781
5	−7.01707	19.8444	465.447	44.3322	189.689	674.807
6	−6.63309	15.0121	463.313	44.144	190.563	651.917
7	−5.4117	6.02635	456.832	43.5588	193.322	585.323
8	−7.99167	8.24191	469.608	44.7012	188.001	725.545
9	−5.08561	16.6683	455.502	43.4409	193.89	569.634
10	−5.83443	17.5422	459.465	43.8038	192.162	609.211
11	−7.85428	16.3007	469.213	44.6661	188.16	720.54
12	−5.45001	12.9046	457.207	43.5922	193.163	588.092
13	−6.19194	14.5563	461.087	43.9459	191.49	627.597
14	−7.35972	10.1741	466.718	44.4435	189.176	690.951
15	−7.63388	7.02841	467.94	44.5529	188.675	704.887
16	−6.36219	19.2626	462.214	44.047	191.016	638.197
17	−6.38987	15.6857	462.17	44.0421	191.039	638.798
18	−7.18076	8.90125	465.814	44.3669	189.53	680.52
19	−7.12625	7.2617	465.543	44.3405	189.651	676.96
20	−7.65774	10.7915	468.151	44.5723	188.587	707.731
21	−6.53342	18.5399	463.018	44.1149	190.697	647.39
22	−6.88474	13.6588	464.505	44.2472	190.082	665.287
23	−5.6624	7.69491	458.229	43.6923	192.691	598.825
24	−6.0518	16.9048	460.527	43.8954	191.728	620.739
25	−6.55528	18.9934	463.161	44.1285	190.634	648.726
26	−7.23112	9.87364	466.072	44.3861	189.439	683.325
27	−7.46849	17.9243	467.432	44.5068	188.885	698.968
28	−5.93787	9.35389	459.676	43.8235	192.07	613.299
29	−6.01876	10.9427	460.157	43.862	191.885	617.906
30	−6.7875	12.4805	463.993	44.2039	190.284	659.834
31	−5.13016	11.9619	455.496	43.4402	193.893	571.456
32	−6.91472	13.2935	464.643	44.2642	190.006	666.854
33	−5.33619	15.4007	456.756	43.5573	193.333	582.604
34	−7.77015	11.3675	468.664	44.6162	188.386	714.23
35	−5.56969	6.63071	457.743	43.6484	192.9	593.756

3.3.2. RSM Model and Optimization

RSM is an experimental design method that combines statistics and mathematical modeling. It can describe the relationship between input variables and output responses using response surface equations. The basic principle of RSM is to use a low-order polynomial function to approximate a true, unknown continuous surface function within a finite experimental range. By fitting an explicit mathematical model using a small number of carefully designed experimental points, RSM is used to analyze the effects of factors, predict responses, and identify optimal operating conditions. After conducting DOE, regression analysis can be used to fit the experimental data, thereby constructing a response surface and then using analysis of variance (ANOVA) to evaluate the applicability and statistical significance of the model [46].

Using Design Expert software, the results of the 35 sets of experiments in the DOE were analyzed to obtain mathematical regression models for pressure, power, BSFC, ITE, and NO_x. The regression equations obtained based on the coded factors are shown below:

$$Power = 424.08009 - 6.79919x + 0.013383\text{y} + 0.005758xy - 0.135849x^2 + 0.002223y^2 \quad (17)$$

$$ITE = 40.51670 - 0.645089x + 0.002136y + 0.000717xy - 0.014965x^2 + 0.000211y^2 \quad (18)$$

$$BSFC = 208.40135 + 3.28431x - 0.010866y - 0.003479xy + 0.090427x^2 - 0.000985y^2 \quad (19)$$

$$NO_x = 339.27683 - 40.87984x - 0.451726y - 0.087682xy + 0.943688x^2 + 0.004293y^2 \quad (20)$$

where x is DIT (°CA BTDC), and y is DID (°CA).

To verify the adequacy and statistical significance of the fitted models, analysis of variance (ANOVA) was performed. The fitting quality of the response surface is mainly composed of three evaluation indicators, namely the coefficient of determination (R^2), the adjusted coefficient (Adj·R^2), and the predicted coefficient (Pre·R^2). R^2 measures the proportion of total variability explained by the model. Adj·R^2 corrects R^2 for the number of predictors. Pre·R^2 assesses the model's predictive capability. The closer these three coefficients are to 1, the better the quality of the fitted response surface. As shown in Tables 8 and 9, the R^2, Adj·R^2 and Pre·R^2 are higher than 0.99, which indicates that the quality of response surface is satisfactory.

Table 8. Analysis of variance results for the response surface models of power and ITE.

Source	Power		ITE	
	F-Value	*p*-Value	F-Value	*p*-Value
Model	208,827.18	<0.0001	58,282.43	<0.0001
x	991,905.27	<0.0001	276,404.12	<0.0001
y	983.51	<0.0001	264.58	<0.0001
xy	19.53	0.0001	10.68	0.0028
x2	424.46	<0.0001	181.45	<0.0001
y2	59.99	<0.0001	19.05	0.0001
R^2	0.99997		0.9999	
Adj·R^2	0.99997		0.9999	
Pred·R^2	0.99995		0.9998	

ANOVA was then performed to test the model, where the F-value and p-value can be used to assess the validity of the model. The F-value reflects the significance of the model, while the p-value is typically compared to a given significance level (commonly 0.05 or 0.01). Generally, a p-value < 0.05 denotes a significant influence between the factor and target, while a p-value < 0.01 indicates a more strongly significant influence. Based on the results in Tables 8 and 9, it can be seen that the p-values for power, BSFC, ITE, and NO_x are all less than 0.05, indicating that the linear terms (x and y), interaction term (xy), and quadratic terms (x^2 and y^2) all exhibited significant effects on power, ITE, BSFC, and NO_x emissions. Furthermore, according to Equations (17)–(20), the absolute values of the coefficients follow the order of x > x^2 > y > xy > y^2. This indicates that the independent variable x is the dominant factor affecting engine performance and emissions, with both its linear and quadratic terms exerting substantially greater influences on the response variables than those of y. The statistically significant interaction term (xy) suggests the existence of a coupling effect between the two control parameters, whereas the quadratic nonlinearity associated with y is relatively weak. Variable x exhibits a clear trade-off between performance and emissions: advancing DIT can significantly suppress NO_x formation but simultaneously reduces power output and thermal efficiency while increasing fuel consumption. In contrast, increasing y can provide modest but concurrent improvements in power performance, fuel economy, and emission characteristics. For NO_x emissions, the significant xy term in Equation (20) indicates that the effect of DIT is dependent on the selected DID, demonstrating a coupled influence of the two injection parameters on NO_x formation. Advancing DIT generally promotes earlier combustion phasing and increases the in-cylinder temperature, which tends to increase NO_x emissions. However, extending DID distributes the heat release process over a longer crank angle duration and alleviates local temperature peaks, thereby mitigating the NO_x increase induced by advanced DIT. The relatively small coefficient of the y^2 term suggests that the nonlinear influence of DID on NO_x is limited within the investigated range.

Table 9. Analysis of variance results for the response surface models of BSFC and NO_x.

Source	BSFC		NO_x	
	F-Value	*p*-Value	F-Value	*p*-Value
Model	65,029.35	<0.0001	699,114.85	<0.0001
x	307,889.43	<0.0001	3,342,405.33	<0.0001
y	295.72	<0.0001	1345.19	<0.0001
xy	12.81	0.0012	126.46	<0.0001
x2	337.88	<0.0001	571.98	<0.0001
y2	21.16	<0.0001	6.25	0.0184
R^2	0.9999		0.99999	
Adj·R^2	0.9999		0.99999	
Pred·R^2	0.9998		0.99999	

Figure 19 shows the response surfaces of DIT and DID on power, ITE, BSFC, and NO_x. As DIT advanced and DID extended, power and ITE showed an upward trend, while BSFC showed a downward trend. However, NO_x emissions increased. Therefore, it is necessary to use optimization algorithms to optimize power, economy and emissions.

The Design Optimization module in DOE-POST can be used to optimize power, ITE, BSFC, and NO_x. The optimization algorithms include GA Standard optimization and Multi-Objective Pareto optimization. GA Standard was used for optimization. The maximum number of generations was set to 1000. Convergence was defined as occurring when the metrics remain unchanged after 200 generations. The sample size and mutation rate were set to 20 and 10%. The optimization objectives were maximum power, maximum ITE, minimum BSFC, and minimum NO_x emissions. Figure 19 demonstrates that the improvement of power output and fuel economy is inherently accompanied by a trade-off with NO_x emissions. Therefore, the ideal optimization objectives cannot be achieved simultaneously within the operating range investigated. Consequently, the optimization performed in this study should be regarded as a decision-support process rather than a search for a unique global optimum. To accommodate different engineering priorities, two recommended optimization schemes were proposed based on the response surface model. The maximum cylinder pressure when the NGSR is 0 was set as the constraint for optimizing the diesel–NG dual-fuel engine.

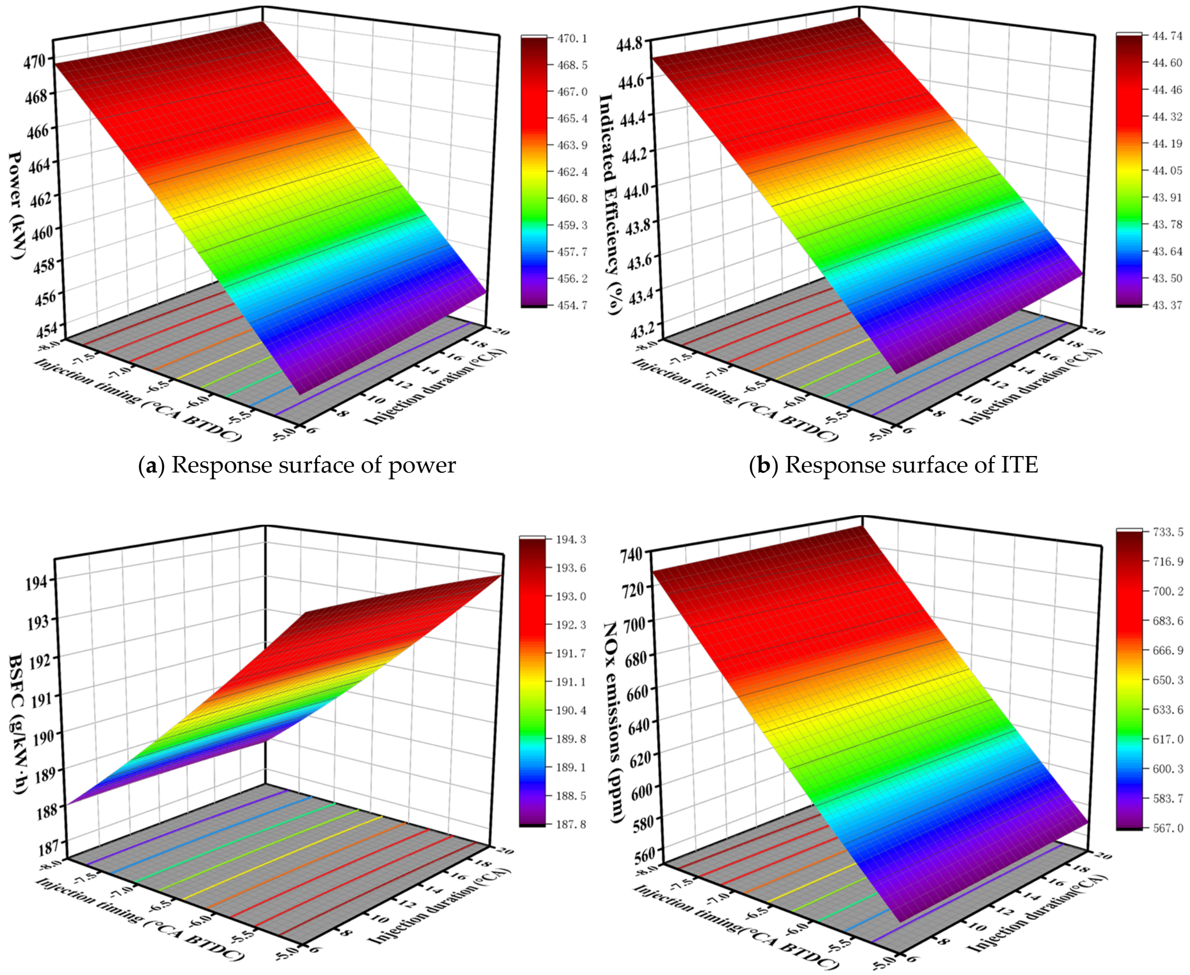

(**a**) Response surface of power (**b**) Response surface of ITE

(**c**) Response surface of BSFC (**d**) Response surface of NO_x emissions

Figure 19. Response surfaces of diesel injection timing and diesel injection duration on (**a**) power, (**b**) indicated efficiency, (**c**) brake-specific fuel consumption, and (**d**) NO_x emissions at 100% engine load.

The optimization results are shown below:

When engine performance and fuel economy were prioritized, NO_x emissions were treated as a secondary consideration, automatic optimization was performed based on the above settings, and the final scheme was as follows: DIT = −7.521994 °CA and DID = 10.545455 °CA. The results of the response surface prediction are shown in Table 10. The prediction results have a certain degree of error, so the final scheme needs to be substituted back into the simulation model for calculation to obtain accurate results. The approximate values for the final scheme are as follows: DIT = −7.52 °CA and DID = 10.55 °CA. The results obtained from the simulation model calculation were compared with the response surface prediction results in Table 10. The recommended value of DIT = −7.52 °CA was obtained directly from the GA optimization process rather than being manually selected. During the optimization, the maximum cylinder pressure under pure diesel operation was imposed as a constraint. Further advancing the injection timing tended to increase the peak cylinder pressure and could violate the prescribed pressure limit. Consequently, the optimization converged to DIT = −7.52 °CA as the preferred operating condition rather than a more advanced injection timing. Under the adopted optimization strategy, this operating condition provided the most favorable overall performance in terms of power output, ITE, BSFC, and NO_x emissions.

Table 10. Comparison of response surface prediction and simulation calculation in case 1.

	Response Surface Prediction	Simulation Model Calculation	Relative Error
Power (kW)	467.441255	467.40616	0.008%
ITE (%)	44.511002	44.505768	0.012%
BSFC (g/kW·h)	188.86205	188.89099	0.015%
NO_x (ppm)	699.272435	699.4441	0.025%

As can be seen from the table, the results of the response surface prediction show very little error compared to the simulation calculation results, indicating that the response surface model has excellent fitting performance and high reliability, enabling precise prediction of the engine model results.

The optimal scheme was compared with the results when the NGSR was 0, and the comparison results are displayed in Figure 20.

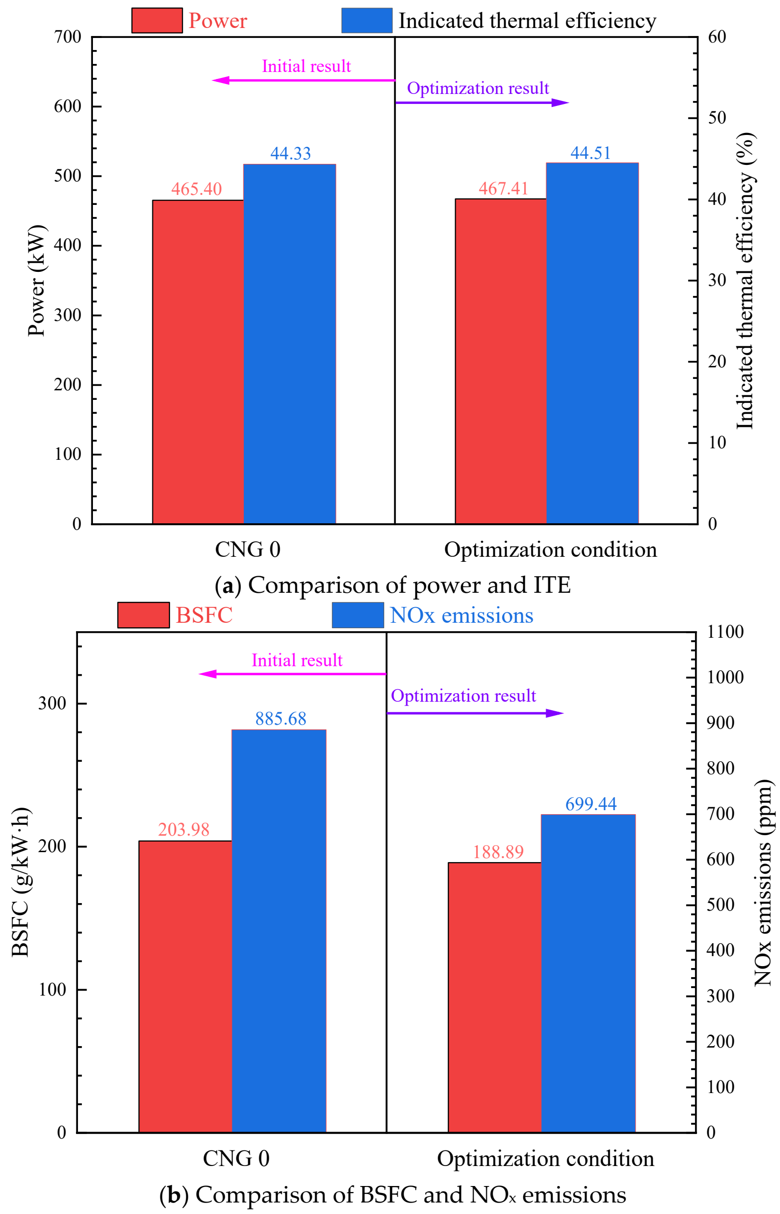

Figure 20. Comparison between pure diesel mode and optimized dual-fuel case 1 in terms of (**a**) power and indicated thermal efficiency and (**b**) brake-specific fuel consumption and NO_x emissions.

By optimizing the DIT and DID, compared to pure diesel mode, power increased by 0.431%, ITE increased by 0.396%, BSFC decreased by 7.397%, and NO_x emissions decreased by 27.027%. Therefore, while maintaining power performance, the diesel–NG dual-fuel engine can reduce fuel consumption and significantly reduce NO_x emissions, demonstrating the advantages of dual fuel.

For applications where stricter emission control is required, an alternative optimization scheme was developed with greater emphasis on NO_x reduction. When the optimization objective focused on emissions as the priority, automatic optimization was performed based on the above settings, and the final scheme was as follows: DIT = −5.002933 °CA and DID = 6.013685 °CA. Similarly, the final scheme was approximated, with DIT = −5 °CA and DID = 6.01 °CA substituted into the simulation model. The results are shown in Table 11.

Table 11. Comparison of response surface prediction and simulation calculation in case 2.

	Response Surface Prediction	Simulation Model Calculation	Relative Error
Power (kW)	454.683414	454.6254	0.013%
ITE (%)	43.368354	43.3694	0.002%
BSFC (g/kW·h)	194.237216	194.23958	0.001%
NO_x (ppm)	564.492524	564.15247	0.06%

From the table, the results of response surface prediction show very little error compared to the simulation calculations, further proving the high predictive accuracy of the response surface model.

Similarly, comparing the optimized results with the pure diesel mode, the comparison results are displayed in Figure 21. Power decreased by 2.315%, ITE decreased by 2.167%, and power performance decreased significantly, but BSFC decreased by 4.775% and NO_x emissions decreased by 36.303%, indicating that NO_x emissions were optimized to a considerable extent. Compared with the performance-oriented scheme, this strategy achieved a substantially lower NO_x emission level at the expense of a slight reduction in power output and fuel economy. Such a scheme may be more suitable for future operating scenarios with increasingly stringent emission regulations.

One limitation of the present study is that the RSM models were constructed based on simulation results obtained at NGSRs of 50% and 100% loads, with DIT ranging from 8 to 5 °CA BTDC and DID ranging from 6 to 20 °CA. Within this investigated range, the response surface models demonstrated good predictive capability and accurately represented the simulation results generated by the validated GT-SUITE v2016 model. However, the predictive accuracy of these models outside the investigated operating and parameter range has not been verified and may require further calibration and validation before practical application. In addition, it should be noted that the proposed dual-fuel combustion model was indirectly validated by comparison with published experimental heat release characteristics because dedicated dual-fuel experimental data for the investigated engine were unavailable. Although the predicted heat release profile agrees well with the published combustion behavior under similar combustion strategies and operating conditions, a direct quantitative validation against experimental measurements for the same engine could not be performed. Therefore, the optimized DIT and DID values obtained in this study should be regarded as engineering guidance for future diesel–natural gas dual-fuel experimental investigations rather than universally applicable optimal solutions. Future work will focus on conducting dual-fuel engine experiments to validate the simulation predictions and further assess the applicability of the proposed optimization strategy under practical operating conditions.

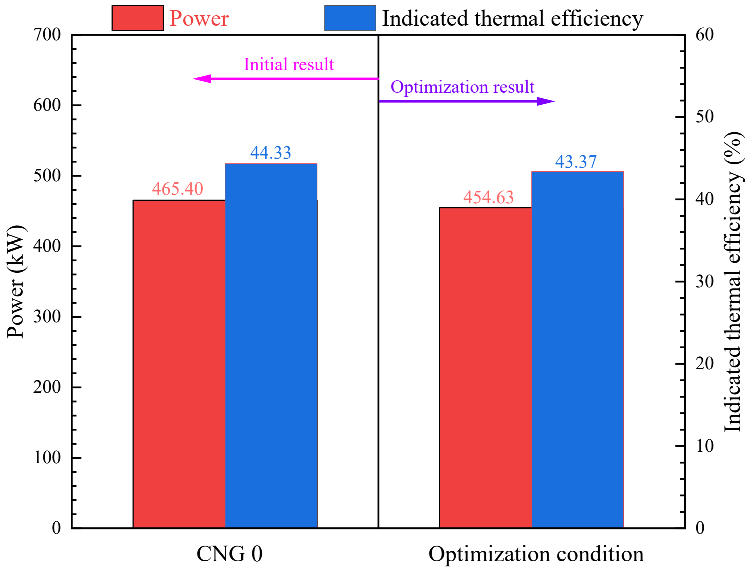

(**a**) Comparison of power and ITE

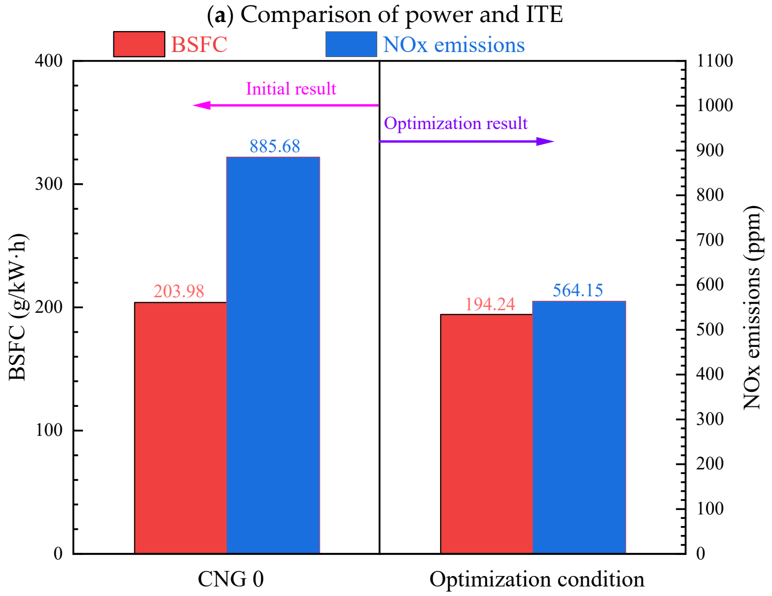

(**b**) Comparison of BSFC and NO_x emissions

Figure 21. Comparison between pure diesel mode and emission-optimized dual-fuel case 2 in terms of (**a**) power and indicated thermal efficiency and (**b**) brake-specific fuel consumption and NO_x emissions.

4. Conclusions

This study conducted a numerical simulation study on the combustion and emission characteristics of diesel–NG dual-fuel engines, mainly investigating the effects of different NGSR and diesel injection strategies on the power, economy and emissions of engines under different loads. The primary conclusions are summarized as follows:

1. The dual-fuel combustion mode effectively improves both engine combustion characteristics and emission performance, while maintaining power output and substantially enhancing fuel economy.
2. With the increase in the NGSR, the cylinder pressure decreased at 100% and 75% loads and increased at 50% and 25% loads. At 100%, 75%, 50% and 25% loads, the temperature inside the cylinder showed a tendency to decrease, and the power and ITE decreased slightly, but the economy and emissions were well improved. Compared to CNG50 and CNG0, BSFC decreased by 5.63%, 4.60%, 2.98%, and 1.83%, respectively,

NO_x emissions decreased by 32.68%, 36.41%, 37.90%, and 38.99%, respectively, and CO_2 emissions decreased by 12.32%, 12.48%, 14.39%, and 14.34%, respectively.

3. As the DIT was advanced, both cylinder pressure and temperature increased, and power and ITE had a large improvement. Under four loads, comparing IT 17 °CA BTDC and 5 °CA BTDC, power increased by 8.29%, 9.76%, 13.38%, and 16.51%, and ITE increased by 7.69%, 8.77%, 11.46%, and 12.77%, respectively. BSFC decreased, but this also led to an increase in NO_x emissions.
4. Using the DOE module in GT-SUITE v2016 to establish response surfaces and optimize performance at an NGSR of 50% and 100% loads, the established response surfaces exhibited high predictive accuracy, enabling reliable and precise predictions of engine performance. After automatic optimization via genetic algorithms, the optimized power output was 0.431% higher than the pure diesel mode, ITE was 0.396% higher, BSFC was reduced by 7.397%, and NO_x emissions were reduced by 27.027%. Through DOE and response surface methodology, engine performance can be predicted, thereby finding the optimal parameters under different operating conditions.
5. This study has established a comprehensive one-dimensional simulation modeling method for dual-fuel engines, providing a modeling framework for future research. It investigated the effects of NSGR and DIT on engine performance, offering data support for a deeper understanding of the dual-fuel combustion process. By combining GT-SUITE v2016 simulation with DOE for multi-objective optimization of injection parameters, this study achieved a balance between engine performance and NO_x emissions, thereby providing an efficient technical approach for multi-objective optimization of similar engines. In future research, studies could be conducted under dynamic operating conditions involving a wider range of engine loads and speeds. Additionally, engine bench tests could be performed to validate the findings, thereby further enhancing the comprehensiveness of the research conclusions.

Author Contributions: Conceptualization, J.E. and Y.M.; methodology, J.E.; software, C.K. and X.C.; validation, C.K. and X.C.; formal analysis, J.E., C.K., X.C., S.Z. and Y.M.; investigation, J.E., C.K., X.C., S.Z. and Y.M.; resources, C.K.; data curation, J.E., C.K., X.C., S.Z. and Y.M.; writing—original draft preparation, C.K., X.C.; writing—review and editing, J.E., S.Z. and Y.M.; visualization, C.K. and X.C.; supervision, J.E.; project administration, J.E. and Y.M.; funding acquisition, J.E. All authors have read and agreed to the published version of the manuscript.

Funding: This work was supported by the Guangxi Science and Technology Major Project (Grant number LT2504240010, GuikeAA23062006 and GuikeAA23023014).

Data Availability Statement: The original contributions presented in the study are included in the article, further inquiries can be directed to the corresponding author.

Conflicts of Interest: Author Chuanfu Kou was employed by the company Guangxi Yuchai Machinery Co., Ltd. The remaining authors declare that they have no conflicts of interest regarding the publication of this paper.

Nomenclature

NG	Natural gas
NGSR	Natural gas substitution rate
DIT	Diesel injection timing
IT	Injection timing
BTDC	Before top dead center
CA	Crank angle
NOx	Nitrogen oxide
CO	Carbon monoxide

CO2	Carbon dioxide
HC	Hydrocarbon
PM	Particulate matter
PPM	Parts per million
CNG0	Natural gas substitution rate is 0%
BSFC	Brake-specific fuel consumption
ITE	Indicated thermal efficiency
HRR	Heat release rate
CFD	Computational fluid dynamic
HPDI	High-pressure direct injection
DPI	Diesel pilot ignition
EGR	Exhaust gas re-circulation
DOE	Design of experiments
ANOVA	Analysis of variance
SOC	Start of combustion
DID	Diesel injection duration
RSM	Response surface methodology
CNG50	Natural gas substitution rate is 50%

References

1. Tan, Y.; Kou, C.; Ning, D.; E, J.; Feng, C. Effects of the structure parameters on methane emission control of an adsorptive three-way catalytic converter during cold start of the heavy-duty natural gas engines. *Energy* **2025**, *317*, 134654. [CrossRef]
2. Kou, C.; Zeng, S.; Chen, X.; E, J.; Ma, Y. Effects of air–fuel ratio on combustion performance enhancement and emission reduction of the methanol–diesel dual-fuel engine. *Can. J. Chem. Eng.* 2026, *early view*. [CrossRef]
3. Zheng, J.; Hao, Z.; Wang, D.; Di, Y.; Peng, H.; Wu, T.; Miao, X. Effect of double-layer hole nozzle with narrow spray angle on combustion and emissions in dual-fuel natural gas engine. *Fuel* **2022**, *314*, 123090. [CrossRef]
4. Zhang, B.; Xia, J.; Zhang, F.; Shen, Z.; Zhang, F. Investigation on the effect of recuperator design on the supercritical carbon dioxide power cycle for hypersonic vehicles. *Aerosp. Sci. Technol.* **2026**, *177*, 112314. [CrossRef]
5. Li, J.; E, J.; Ding, J.; Cai, L.; Luo, B. Investigation on thermophotovoltaic performance enhancement of the hydrogen fueled micro combustors with the center-cleared twisted tapes for micro-thermophotovoltaic system. *Appl. Therm. Eng.* **2025**, *264*, 125483. [CrossRef]
6. Li, J.; E, J.; Ding, J.; Cai, L.; Luo, B. Effects of deformed twisted tapes on thermal performance enhancement of hydrogen fueled micro combustor for micro-thermophotovoltaic system. *Appl. Therm. Eng.* **2025**, *264*, 125413. [CrossRef]
7. Park, H.; Shim, E.; Bae, C. Improvement of combustion and emissions with exhaust gas recirculation in a natural gas-diesel dual-fuel premixed charge compression ignition engine at low load operations. *Fuel* **2019**, *235*, 763–774. [CrossRef]
8. Liu, J.; Zhao, W.; Zhang, X.; Ji, Q.; Ma, H.; Sun, P.; Wang, P. Optimizing combustion and emissions in natural gas/diesel dual-fuel engine with pilot injection strategy. *Therm. Sci. Eng. Prog.* **2024**, *48*, 102418. [CrossRef]
9. Wang, W.; Mai, Z.; Yao, X.; Tang, C.; Huang, Z. Towards optimized excess air ratio and substitution rate for a dual fuel HPDI engine. *Appl. Therm. Eng.* **2024**, *253*, 123797. [CrossRef]
10. Papagiannakis, R.; Hountalas, D.; Rakopoulos, C. Theoretical study of the effects of pilot fuel quantity and its injection timing on the performance and emissions of a dual fuel diesel engine. *Energy Convers. Manag.* **2007**, *48*, 2951–2961. [CrossRef]
11. Wu, Z.; Han, Z. Micro-GA optimization analysis of the effect of diesel injection strategy on natural gas-diesel dual-fuel combustion. *Fuel* **2020**, *259*, 116288. [CrossRef]
12. Pinto, G.M.; Souza, T.; Costa, R.; Roque, L.; Frez, G.V.; Vidigal, L.; Perez-Rangel, M.; Coronado, C. Hydrogen and CNG dual-fuel operation of a 6-Cylinder CI engine fueled by HVO and diesel: Emissions, efficiency, and combustion analyses. *Int. J. Hydrogen Energy* **2025**, *111*, 407–432. [CrossRef]
13. Saaidia, R.; Hamdi, F.; Krotli, M.; Bouabidi, A.; Cuce, E.; Koten, H.; Miraoui, I. Performance and emission characteristics of hydrogen enriched CNG in a dual fuel diesel engine: An experimental and numerical research. *Renew. Energy* **2025**, *241*, 122387. [CrossRef]
14. Robbio, D.R.; Mancaruso, E. Hydrogen combustion analysis via infrared and visible optical diagnostics combined with CFD in a dual fuel engine at low load. *Int. J. Hydrogen Energy* **2024**, *81*, 418–435. [CrossRef]
15. Zhang, C.; Song, J. Experimental study of co-combustion ratio on fuel consumption and emissions of NG-diesel dual-fuel heavy-duty engine equipped with a common rail injection system. *J. Energy Inst.* **2016**, *89*, 578–585. [CrossRef]

16. Wei, L.; Geng, P. A review on natural gas/diesel dual fuel combustion, emissions and performance. *Fuel Process. Technol.* **2016**, *142*, 264–278. [CrossRef]
17. Mirosław, K.; Grzegorz, S.; Janusz, C. Experimental assessment of the impact of replacing diesel fuel with CNG on the concentration of harmful substances in exhaust gases in a dual fuel diesel engine. *Energies* **2022**, *15*, 4563. [CrossRef]
18. Sudhir, K.P.; Ashish, N.; Varun, G. Optimization of EGR effects on performance and emission parameters of a dual fuel (Diesel+CNG) CI engine: An experimental investigation. *Fuel* **2021**, *291*, 120183. [CrossRef]
19. Lee, S.; Kim, C.; Lee, S.; Lee, J.; Kim, J. Diesel injector nozzle optimization for high CNG substitution in a dual-fuel heavy-duty diesel engine. *Fuel* **2020**, *262*, 116607. [CrossRef]
20. Wang, Z.; Fu, X.; Wang, D.; Xu, Y.; Du, G.; You, J. A multilevel study on the influence of natural gas substitution rate on combustion mode and cyclic variation in a diesel/natural gas dual fuel engine. *Fuel* **2021**, *294*, 120499. [CrossRef]
21. Yousefi, A.; Birouk, M. Investigation of natural gas energy fraction and injection timing on the performance and emissions of a dual-fuel engine with pre-combustion chamber under low engine load. *Appl. Energy* **2017**, *189*, 492–505. [CrossRef]
22. Papagiannakis, R.; Hountalas, D. Experimental investigation concerning the effect of natural gas percentage on performance and emissions of a DI dual fuel diesel engine. *Appl. Therm. Eng.* **2003**, *23*, 353–365. [CrossRef]
23. Ahmad, N.; Babu, M.K.G.; Ramesh, A. Experimental investigations of different parameters affecting the performance of a CNG-Diesel dual fuel engine. *SAE Trans.* **2005**, *114*, 1620–1629.
24. Lee, C.; Pang, Y.; Wu, H. An optical investigation of substitution rates on natural gas/diesel dual-fuel combustion in a diesel engine. *Appl. Energy* **2020**, *261*, 114455. [CrossRef]
25. Shu, J.; Fu, J.; Zhang, Y.; Xie, M.; Liu, J.; Liu, J.; Zeng, D. Influences of natural gas energy fraction on combustion and emission characteristics of a diesel pilot ignition natural gas engine based on a reduced chemical kinetic model. *Fuel* **2020**, *261*, 116432. [CrossRef]
26. Zhou, H.; Li, X.; Lee, C. Investigation on soot emissions from diesel-CNG dual-fuel. *Int. J. Hydrogen Energy* **2019**, *44*, 9438–9449. [CrossRef]
27. Cheenkachorn, K.; Poompipatpong, C.; Choi, G. Performance and emissions of a heavy-duty diesel engine fueled with diesel and LNG (liquid natural gas). *Energy* **2013**, *53*, 52–57. [CrossRef]
28. Lounici, M.; Loubar, K.; Tarabet, L.; Balistrou, M.; Niculescu, D.; Tazerout, M. Towards improvement of natural gas-diesel dual fuel mode: An experimental investigation on performance and exhaust emissions. *Energy* **2014**, *64*, 200–211. [CrossRef]
29. Chen, W.; Pan, J.; Liu, Y.; Fan, B.; Liu, H.; Otchere, P. Numerical investigation of direct injection stratified charge combustion in a natural gas-diesel rotary engine. *Appl. Energy* **2019**, *233*, 453–467. [CrossRef]
30. Abdelaal, M.; Hegab, A. Combustion and emission characteristics of a natural gas-fueled diesel engine with EGR. *Energy Convers. Manag.* **2012**, *64*, 301–312. [CrossRef]
31. Neeraj, K.; Bharat, B.A.; Sagar, M. Environmental impact evaluation of diesel engine fuelled with CNG. *Arch. Environ. Prot.* **2023**, *49*, 79–84. [CrossRef]
32. Pankaj, S.S.; Nitin, M.S.; Subhash, L. Analysis of a combustion, performance and emission characteristics of a CNG-B20 fuelled diesel engine under dual fuel mode. *Carbon-Sci. Technol.* **2016**, *8*, 52–59.
33. Ryu, K. Effects of pilot injection timing on the combustion and emissions characteristics in a diesel engine using biodiesel-CNG dual fuel. *Appl. Energy* **2013**, *111*, 721–730. [CrossRef]
34. Wang, W.; Tang, C.; Huang, Z. Diesel-natural gas dual fuel injection strategy effects on engine ignition delay and cylinder pressure evolution. *Case Stud. Therm. Eng.* **2024**, *53*, 103795. [CrossRef]
35. Wang, Z.; Zhang, F.; Xia, Y.; Wang, D.; Xu, Y.; Du, G. Combustion phase of a diesel/natural gas dual fuel engine under various pilot diesel injection timings. *Fuel* **2021**, *289*, 119869. [CrossRef]
36. Li, M.; Wu, H.; Zhang, T.; Shen, B.; Zhang, Q.; Li, Z. A comprehensive review of pilot ignited high pressure direct injection natural gas engines: Factors affecting combustion, emissions and performance. *Renew. Sustain. Energy Rev.* **2020**, *119*, 109653. [CrossRef]
37. Shu, J.; Fu, J.; Liu, J.; Zhang, L.; Zhao, Z. Experimental and computational study on the effects of injection timing on thermodynamics, combustion and emission characteristics of a natural gas(NG)-diesel dual fuel engine at low speed and low load. *Energy Convers. Manag.* **2018**, *160*, 426–438. [CrossRef]
38. Roussos, G.P.; Sundar, R.K.; Dimitrios, C.R.; Kayyan, K.S.; Constantine, D.R. A combined experimental and theoretical study of diesel fuel injection timing and gaseous fuel/diesel mass ratio effects on the performance and emissions of natural gas-diesel HDDI engine operating at various loads. *Fuel* **2017**, *202*, 675–687.
39. Yang, B.; Zeng, K. Effects of natural gas injection timing and split pilot fuel injection strategy on the combustion performance and emissions in a dual-fuel engine fueled with diesel and natural gas. *Energy Convers. Manag.* **2018**, *168*, 162–169. [CrossRef]
40. Yang, B.; Wang, L.; Ning, L.; Zeng, K. Effects of pilot injection timing on the combustion noise and particle emissions of a diesel/natural gas dual-fuel engine at low load. *Appl. Therm. Eng.* **2016**, *102*, 822–828. [CrossRef]
41. Yousefi, A.; Guo, H.; Birouk, M. Effect of diesel injection timing on the combustion of natural gas/diesel dual-fuel engine at low-high load and low-high speed conditions. *Fuel* **2019**, *235*, 838–846. [CrossRef]

42. Yousefi, A.; Birouk, M.; Guo, H. An experimental and numerical study of the effect of diesel injection timing on natural gas/diesel dual-fuel combustion at low load. *Fuel* **2017**, *203*, 642–657. [CrossRef]
43. Bambang, S.; Atok, S.; Ary, B.K.P.; Dori, Y.; Jose, S. Optimization of pilot diesel injection timing on load variation dual fuel diesel-CNG engine on combustions and emissions characteristics. *Int. Rev. Mech. Eng.* **2019**, *13*, 58–69. [CrossRef]
44. Liu, J.; Guo, Q.; Guo, J.; Wang, F. Optimization of a diesel/natural gas dual fuel engine under different diesel substitution ratios. *Fuel* **2021**, *305*, 121522. [CrossRef]
45. Oishy, M.M.; Mustak, R.; Bakchi, S. Influence of combustion modes on the various characteristics of a Natural Gas-Diesel dual fuel CI engine. *Next Res.* **2025**, *2*, 100504. [CrossRef]
46. Wang, H.; Li, E.; Guang, L. Optimization of drawbead design in sheet metal forming based on intelligent sampling by using response surface methodology. *J. Mater. Process. Technol.* **2008**, *206*, 45–55. [CrossRef]